



Title	Temporal Dynamics of Surround Suppression in the Primary Visual Cortex
Author(s)	石川, 理子
Citation	大阪大学, 2008, 博士論文
Version Type	VoR
URL	https://hdl.handle.net/11094/49302
rights	
Note	

The University of Osaka Institutional Knowledge Archive : OUKA

<https://ir.library.osaka-u.ac.jp/>

The University of Osaka

Doctoral Thesis

**Temporal Dynamics of Surround Suppression
in the Primary Visual Cortex**

初期視覚野における刺激布置に依存した反応修飾

AYAKO ISHIKAWA

**Graduated school of Frontier Biosciences,
Osaka University**

石川 理子

大阪大学大学院生命機能研究科

March 2008

Abstract	1
Section 1. Introduction	2
1.1. Sensory systems.....	2
1.2. Visual systems	2
1.3. What is meaningful visual information for us?.....	3
1.4. The purpose of this study.....	4
Section 2. Surround suppression of V1 cells: electrophysiology in cat V1	6
2.1. Introduction.....	
2.1.1. Visual pathway.....	6
2.1.2. Classical receptive field of V1 neurons.....	7
2.1.3. Surround suppression of V1 neurons.....	7
2.1.4. Properties of surround suppression of V1 neurons.....	10
2.1.5. Possible anatomical substrate.....	12
2.1.6. Functional roles of surround suppression.....	15
2.1.7. The aim of this experiments.....	16
2.2. Methods.....	18
2.2.1. Materials.....	18
2.2.2. Preparations.....	18
2.2.3. Physiological recording and visual stimulation.....	19
2.2.4. Data analysis.....	21
2.3. Results.....	23
2.3.1. Spatiotemporal properties of surround suppression.....	23
2.3.2. Temporal characteristics of SF tuning in surround suppression.....	28
2.3.3. Temporal characteristics of SF tuning of CRF response.....	35
2.3.4. Comparison of SF tuning between CRF responses and surround suppression.....	42
2.4. Discussion.....	44
2.3.1. Properties of surround modulation of V1 cells.....	44
2.3.2. Underlying mechanisms of surround modulation of V1 cells.....	48
2.3.3. Functional rule of surround modulation on V1 cells.....	50
Section 3. Metacontrast: psychophysical study in human	52
3.1. Introduction.....	52
3.1.1. Psychophysical phenomena related to surround modulation.....	52
3.1.2. Metacontrast.....	54
3.2. Methods.....	56
3.2.1. Subjects.....	56

3.2.2. Apparatus and stimuli	56
3.2.3. Procedure.....	57
3.2.4. Experiments.....	59
3.2.5. Data analysis.....	59
3.3. Results.....	62
3.3.1. Experiment 1. Orientation dependency.....	62
3.3.2. Experiment 2: SF dependency.....	65
3.3.3. Experiment3. Contrast dependency.....	68
3.4. Discussion.....	71
3.4.1. Properties of metacontrast.....	71
3.4.2. Possible mechanisms underlying metacontrast.....	72
Section 4. Conclusion.....	77
4.1. Properties of metacontrast and surround modulation in V1.....	77
4.2. Functions of temporal shift of surround modulation.....	78
4.3. Bridging physiology and psychophysics.....	79
Acknowledgments.....	80
References.....	81
Publication list.....	101

Abstract

In the primary visual cortex (V1), the responses of neurons to a stimulus presented in their classical receptive field (CRF) are modulated by another stimulus simultaneously presented in the surround of CRF. Because the modulatory effect is generally suppressive, it is called “surround suppression”. There is a perceptual correlate of this phenomenon called “metacontrast” in which the perception of a particular target is masked by the presentation of another stimulus to the surround with a small delay. In order to clarify the functional organization of the early visual system and also to have an insight into the brain strategy to optimize the efficiency of visual information processing that is appropriate in the behavioral context, I studied both surround suppression neurophysiologically in the cat V1 and metacontrast psychophysically in human. In the first part of the study, I examined temporal properties of surround suppression in V1 neurons. 1) Spatial frequency (SF) tuning of surround suppression changed through time: tuning curve of early response phase ($\leq 50\text{ms}$) was low-pass type, whereas that of late phase ($> 50\text{ms}$) was band-pass type, 2) SF tuning of CRF response also changed through time: the preferred SF shifted from low SF to high SF, and 3) the strength of SF shift of CRF response was smaller than that of surround suppression. In the second part, I examined the spatiotemporal properties of metacontrast using sinusoidal grating as target and mask stimuli. 1) The magnitude of metacontrast was depending on the similarity of stimulus features such as orientation and SF between the target and mask, and 2) at short stimulus-onset-asynchrony (SOA) (0 to ~ 40 ms), metacontrast exhibited strong stimulus specificity and low contrast sensitivity, whereas at long SOA (~ 40 to ~ 80 ms), it exhibited weak stimulus specificity and high contrast sensitivity. These results suggest that surround suppression in V1 and human metacontrast share the similar temporal properties and that the perceptually relevant information processing has been achieved even in the early visual cortex.

Introduction

Our sensory systems process vast amount of information about the environment in the forms of, for examples, light intensities, change in sound pressure, mechanical pressure on the skin, binding of molecules to receptors for olfaction or taste. The information of the environment and animal's own internal state are encoded as the firing pattern and intensity of the responsible neuron population. One of the most interesting questions of neurosciences is how the brain efficiently processes the flood of sensory information to achieve the internal representation of the environment, which is appropriate in the behavioral context.

It is generally accepted that thalamocortical transformation of visual information plays one of the essential roles in optimizing the processing of the brain since the pioneering works of Hubel and Wiesel (1962). To understand cortical function, it is the key question how neurons integrate inputs to produce useful and efficient outputs in the large and fine scale cortical circuitry. In other words, to reveal the rule of integration of inputs by cortical neurons provides the basis for the complex information processing in the cerebral cortex. What is a rule of efficient integration of inputs in neural processing? An appealing hypothesis is that sensory systems reduce the redundancy of inputs to produce more effective representation of the environment (Attneave, 1954; Simoncelli and Olshausen, 2001; Barlow, 1961). It is important to examine this hypothesis, and if it is true, the brain strategies to achieve the reduction of redundancy should be addressed.

1.1. Visual system

Visual system allows to organisms to see. It interprets the information of the distribution of intensity and wavelength of light to represent the environments. The visual images of the natural world have relatively regular statistical structures, that is, they consist of contiguous structures and surfaces of numerous numbers of objects. Neighboring regions have similar composition of light intensity and local features, such as line orientation or spatial frequency, whereas distant regions differ in their visual structure (Dragoi et al., 2002; Reinagel and Zador, 1999; Tolhurst et al., 1992; Field, 1987). It is possible that visual system analyzes information differentially according to the local similarity of visual features. Furthermore, primate, including the human, makes saccadic eye movements several times a second, that bring relevant image regions into fovea. Between saccades, we typically fixate a given location for only 200–300 ms (Yarbus, 1967). During fixation, the portions of a scene that fall within the receptive field (RF) of visual neurons do not change, but before and after saccadic eye movement, the image within the RF changes quickly. Then changes of local features, such as contrast, luminance, orientations, and spatial frequency within the RF typically occur at a rapid pace. It is widely believed that visual systems are optimized for these statistical properties of the visual environment that is rich in a variety of spatiotemporal structures (Simoncelli and Olshausen, 2001; van Hateren and Rauderman, 1998; Field, 1987; Atteave, 1954).

1.2. What is meaningful visual information for us?

One of the important tasks imposed to visual system is quickly encode the incoming visual signals to improve efficiency of information processing. In natural environments, visual scene

includes redundant information that is not necessary for controlling behavior (Atick, 1992). Therefore, the faithful representation of the visual scene is inefficient for controlling behaviors in the continuously changing environment.

What is important and meaningful visual information for us? We perceive visual world as an organized entity of segmented constituent and objects with relationship among each other. These global organizations of visual scene influence our percept of objects. Psychophysical evidence for stimulus-context dependent modulation of visual perception have been accumulated for a number of stimulus attributes, including brightness, color, orientation, spatial frequency, size, depth and so on (Ejima and Takahashi, 1985; Ishikawa et al., 2006; Meese and Hess, 2004; Xing and Heerger, 2000). Perception of an object might be depending not only on the spatial context but also on the temporal context. However, the temporal aspect of stimulus feature-dependent modulation is little known. To reveal how local signals in the visual scene are integrated across space and time to generate global percepts is important for understanding the organizing principles of sensory systems.

1.3. Purpose of this study

The aim of this thesis is to understand how local visual features are integratively processed across space and time by combining an electrophysiological study on the response modulation in the primary visual cortex (V1) of the cat (**Section 2**) and a psychophysical study on the visual masking in human (**Section 3**).

In the Section 2 “Surround suppression of V1 neurons”, I describe the properties of suppressive modulation of visual responses by stimulation of extraclassical receptive field, which is called “surround suppression”, with a particular concern with spatial frequency of

grating stimulus. Characterizing the temporal profile of the surround suppression is essential to understand how neurons in V1 integrate local visual features not only across space but also across time. In the **Section 3 “Psychophysical Study in Human”**, I describe how human perception is affected by spatial and temporal context of stimulus. The psychophysical data in human study on “metacontrast”, in which spatial properties is closely related to neuronal surround suppression of V1, provide property of the integration of local signal at behavior level. Then, in the **Section 4 “Conclusion”**, I discuss on the functional implications of surround suppression in V1 to the perceptual phenomena.

2. Surround suppression of V1 neurons

2.1. Introduction

I examined physiological properties of surround suppression in the primary visual cortex (V1). The surround suppression controlled responses of V1 neurons to the stimulation of the classical receptive field (CRF) depending on the stimulus configuration in the visual field. To clarify the spatio-temporal properties of surround suppression should be essential for understanding the brain strategies for integrating abundant local signals so as to be relevant in spatial and temporal frameworks of visual environment.

2.1.1. Visual pathway

Visual information is first transduced in the retina and provided to cortical visual pathway via lateral geniculate nucleus (LGN). Through hierarchical processing of visual pathway, neurons at higher stage integrate information of larger region of space. Between neurons in each visual area, we could observe difference not only in spatial integration, but also in the spatial and temporal properties of receptive field (RF). For example, neurons in LGN have a classical receptive field (CRF) that consists of an antagonistic organization of a center (CRF center) and a surround within the CRF (CRF surround), whereas neurons in the primary visual cortex (V1) have spatially elongated CRF, which does not have an antagonistic organization like LGN neurons. Selectivity of orientation, spatial frequency (SF) and temporal frequency (TF) also differ between neurons in LGN and V1. That is, LGN neurons exhibit responses with no

much orientation selectivity, low-pass type of SF tuning and higher TF tuning comparing to those of V1 neurons (Rodieck and Stone, 1965; Derrington and Hicks, 1979; So and Shapley, 1979; Kaplan and Shapley, 1982; Hicks et al., 1983; Irvin et al., 1993). These differences depending on the visual areas will be useful to estimate underlying mechanisms of neuronal phenomena, including surround modulation.

2.1.2. Classical receptive field of V1 neurons

The classical receptive field (CRF) of V1, the area that evoked spike response, localizes in the narrow space in the visual field (Hubel and Wiesel, 1958). Neurons in V1 are tuned to particular stimulus features such as orientation, spatial frequency, color, direction of motion, and binocular disparity. There are two typical types of CRF in V1 neurons, simple and complex cells. Receptive field of simple cells have spatially segregated ON- or OFF- subregion, and are suggested to compute a linearly weighted sum for the inputs over space and time like a Gabor function filter. The CRF of complex cells does not have segregated subregions, and because of this, complex cells are insensitive to spatial phase of stimulus. Several studies have shown that structures of CRF in V1, which is spatially localized and tuned orientation and spatial frequency, seems to be useful for having responses to natural visual scene statistically independent (Oja, 1982; Sanger, 1989: using *principal Component analysis*; Common, 1994; Bell and Sejnowski, 1997 using *independent component analysis*). It means that one of the important functional roles of CRFs of V1 neurons is transformation of the incoming visual signals to improve efficiency.

2.1.3. Surround modulation in V1

In V1, the spatial extent of integration by a neuron includes not only its CRF where visual stimuli elicit spike responses, but also the extraclassical receptive field (ECRF), where stimuli don't elicit spike responses, but modulate responses evoked by CRF stimulation (Allman et al., 1985; Gilbert, 1992; Fitzpartick, 2000; Akasaki et al., 2002; Ozeki et al, 2004; Blakemore and Tobin, 1972; Nelson and Frost, 1978; Knierim and Van Essen, 1992; DeAngelis et al., 1994; Sengpiel et al., 1997; Sceniak et al., 1999; Walker et al. 1999, 2000; Akasaki et. al., 2002; Ozeki et. al., 2004). The predominant effect of stimulation of ECRF is the suppression of the response to CRF stimulation. (Blakemore and Tobin, 1972; Nelson and Frost, 1978; Knierim and Van Essen, 1992; DeAngelis et al., 1994; Sengpiel et al., 1997; Sceniak et al., 1999; Walker et al. 1999, 2000; Akasaki et. al., 2002; Ozeki et. al., 2004) rather than facilitation (Maffei and Fiorentini, 1976; Li and Li, 1994; Sillito et al., 1995; Levitt and Lund, 1997; Polat et al., 1998). Surround suppression is observed for a majority of V1 neurons. An electrophysiological study (Akasaki et al., 2000) reported that 65 % of cat V1 neurons showed significant suppression when increasing the diameter of a central grating beyond the CRF. Similar to CRF regions, the surround regions are highly sensitive to the characteristics of the stimuli, such as orientation, spatial frequency and so on. These tuning properties of surround suppression are similar to, but broader than those of the response to CRF stimulation (DeAngelis et al., 1994; Gilbert and Wiesel, 1990).

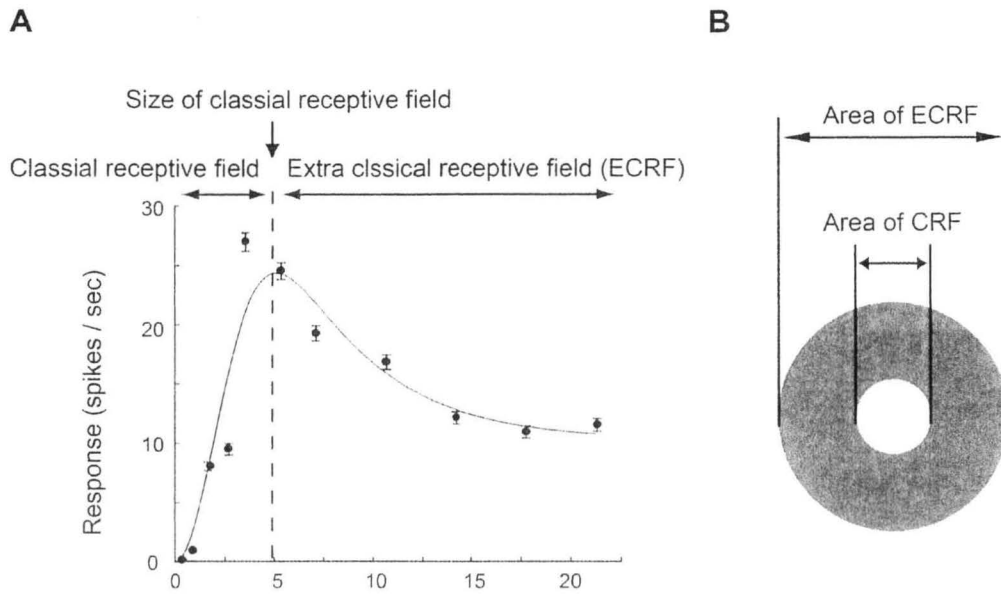


Figure 1.

Classical receptive field and extra classical receptive field. **A**, Size tuning curve of a single neuron. Mean firing rate is plotted against the stimulus diameter. Classical receptive field (CRF) determined as a size, which evokes maximal response (red arrows). **B**, CRF (right gray area) and ECRF (dark gray area).

2.1.4. Properties of surround suppression of V1 neurons

Combined stimulation of CRF and ECRF with systematically changing the parameters of grating stimuli reveals properties of surround modulation. The properties of surround modulation will be useful to estimate underlying mechanisms and know the functional roles.

(1) Size tuning curve

The response of V1 neurons increases when the circular grating patch with appropriate orientation and spatial frequency (SF) is enlarged within CRF, and then decreases when stimulus becomes larger than CRF size (**Fig. 1A**). Stimulus size, which evokes maximal response, is determined as CRF size (**Fig. 1A**, red arrow), and the area outside of CRF, which modulates response to CRF stimulation, is determined as ECRF (**Fig. 1B**). The peak size of the tuning and the proportion of response suppression vary depending on stimulus parameters, such as contrast, orientation and SF. For example, when the low contrast stimulus is used, the CRF size becomes larger than that at high contrast stimulation condition (Sceniak et al., 1999). And when the non-optimally orientated grating is used, the CRF size becomes smaller and the strength of surround suppression becomes larger than that of optimal orientation condition (Xing et al., 2005). These data suggest that spatial summation properties of V1 neurons change depending on stimulus parameter, such as orientation, SF and contrast.

(2) Position of surround stimuli

The spatial extent of ECRF is estimated to be at least 2-5 times larger than the CRF (Li and Li, 1994; Maffei and Fiorentini, 1976). However, some studies (DeAngelis et al., 1994; Walker et al., 1999, 2002) showed that the most suppressive surround region was variably localized in a

small area in ECRF, and often asymmetrically located in ECRF. In cat V1, the most suppressive region is most often found along the preferred orientation axis, at one of the “end-zones” of the RF (Freeman et al., 2001). “End-stop inhibition” and “side stop inhibition”, which are reported more than 40 years ago (Hubel and Wiesel, 1967), are supposed to be due to the presence of inhibitory regions outside the CRF, along the preferred orientation axis (“end-zones”) and on its flanks (“side-bands”).

(3) Orientation / Spatial frequency (SF)

The surround regions are highly sensitive to the characteristics of the CRF stimuli. These stimulus-tuning properties of surround modulation are similar to, but broader than those of CRF response (DeAngelis et al., 1994; Gilbert and Wiesel, 1990). The suppression is generally maximal when CRF and ECRF stimuli have the same orientation and SF, and decreases when the difference in orientation or SF between CRF and ECRF stimuli increased (DeAngelis et al., Knierim and Van Essen, 1992; Levitt and Lund 1997; Li and Li, 1994; Sengpiel et al., 1997; Sillito et al., 1995; Walker et al., 1999; Ozeki et al., 2004). It is generally true that surround suppression makes tuning properties of CRF response sharper than these when CRF is stimulated alone. For examples, the orientation selectivity of V1 neurons increases with an enlargement of stimulus beyond CRF (Chen et al., 2005; Xing et al., 2005), or enhances the “low-pass” property of SF-tuning of V1 neurons (Solomon et al., 2004).

(4) Temporal frequency (TF)

Surround suppression of cat V1 neurons exhibit temporal resolution higher than that of CRF response (Durand et al., 2007). The temporal properties of surround suppression (<15 – 20 Hz) are intermediate between those of CRF response of LGN neurons (<30 Hz) and V1 neurons

(<10 – 15 Hz). The bandwidth of suppression was larger than the bandwidth of CRF responses of V1 neurons.

2.1.5. Possible anatomical substrate

V1 receives its main feedforward inputs from lateral geniculate nucleus (LGN), which receive feedback projection from V1, and sends partially segregated projections to several extrastriate cortical areas, which, in turn, send feedback projections to V1.

Approximately 20 % of neurons and 15 % of synaptic buttons in cat visual cortex contain gamma- aminobutyric acid, which is the major inhibitory neurotransmitter in mammalian cerebral cortex. (Gobbott and Somogyi, 1986; Beaulier and Somogyi, 1990), and every cortical cell receives a rich GABAergic input (Freund et al., 1983). Evidence for a contribution of intracortical inhibition to response properties of V1 neurons has been accumulated from studies employing multiple visual stimuli in the RF (Emerson and Gerstein, 1977; Morrone et al., 1982; Ganz and Felder, 1984; Emerson et al., 1987; Bonds, 1989;) or local inactivation techniques (Eysel et al., 1988, 1990; Crook et al., 1991, 1997; Allison and Bonds, 1994; Sato et al., 1995) and from a number of interacellular recording studies (Creutzfeldt et al., 1974; Innocenti and Fiore, 1974; Sato et al., 1991; Volgushev et al., 1993; Pei et al., 1994).

What are the underlying mechanisms of surround suppression in V1, which seem to integrate information widely distributing in the surround of CRF? It is controversial and, at least, four fundamental projections are suggested for the anatomical. (1) Bottom-up feedforward connection from retina to V1, (2) lateral connection in V1, (3) cortico-thalamic feedback from layer 6 cells in V1 to LGN, and (4) Top-down feedback connections from higher order visual area to V1.

(1) Feedforward bottom-up mechanism

There is evidence for the presence of surround suppression in cat LGN exhibiting contrast-dependency (Sadakane et al. 2006) and orientation tuning (Sillito et al. 1993; Jones et al. 2000; Sun et al. 2004; Naito et al. 2007) which are quantitatively equivalent with those of cortical surround suppression. This raises a possibility that a reduction of feedforward excitatory inputs from LGN to V1 is the primary source of surround suppression in V1. Supporting this notion, a blockade of intracortical inhibition with an iontophoretically administered GABA_A receptor antagonist, bicuculline, in cat V1 did not significantly affect on the strength and orientation tuning of surround suppression (Ozeki et al. 2004).

The size of CRF and ECRF of LGN neurons of cat (Solomon et al., 2002; Bonin et al., 2005) are smaller than those of V1 neurons (Ozeki et al., 2004). However, taking account of the converging thalamo-cortical projection that the arbors of at least 1000 separate thalamic relay cells cover each point of layer 4 of V1 (Freund et al., 1985), a part, at least, of the expansion of CRF and ECRF could be explained.

(2) Intracortical, horizontal connection in V1

Pyramidal cells in the visual cortex are known to send axon collaterals horizontally up to several millimeters (Fisken et al., 1975; Gilbert and Wiesel, 1979) and interconnect functional domains or columns, which process similar stimulus feature (Gilbert, 1983; Ts'o et al., 1986; Hata et al., 1991). There is evidence that neurons in the primary visual cortex exhibit modulatory property of responses according to the stimulus context of inside and outside of the CRF (Kapadia et al., 1995; Sillito et al., 1995; Polat et al., 1998; Akasaki et al., 1998). The long-range horizontal connections are suggested to be one of the structural bases for the integration of visual

information over a wide area in the visual field (see Gilbert, 1992, for review).

Long-range horizontal projection in V1 is a possible candidate of the anatomical substrate for the surround suppression for the integration of wide area in the visual field. Because the predominant effect of surround modulation is suppressive, the excitatory influence of long-range horizontal projection has to be mediated by the inhibitory mechanism in V1. The same argument is also applied for the contribution of top-down projection from higher order cortices to V1. However, the above-mentioned minor role of intracortical inhibition on surround suppression in V1 is contradictory to these mechanisms.

(3) Cortico-geniculate feedback

Feedback projection from layer 6 of V1 to LGN can also exhibit both excitatory influence by direct connection to LGN neurons and inhibitory influence by activations of thalamic reticular neurons or geniculate interneurons. (Sillito and Jones 2002) Corticofugal axons innervate an area in the LGN that extends beyond their retinal-input-recipient area, that is, cortico-geniculate projection innervates both CRF and ECRF of LGN neurons (Murphy and Sillito 1996; Murphy et al. 1999, 2000).

(4) Top-down control from higher visual cortices

There are reports suggesting that surround suppression arises from intracortical inhibition in V1, which is directly driven by top-down feedback projection from higher cortical areas (Bullier et al. 2001; Angelucci et al. 2002; Cavanaugh et al. 2002; Angelucci and Sainsbury 2006). These top-down projections have fast conduction velocity, and catch up with the early part of V1 response with a delay of only a few milliseconds (Hupe et al., 2001)

Angelucci and colleagues (2002, 2006), using anatomical and physiological methods,

reported that surround modulation of the area near CRF, which changes its size contrast-dependent manner, is due to an spatial integration by horizontal connection in V1, whereas surround suppression by a stimulation of far surround area comes from higher visual area, such as V2, V3 and MT. However, these feedback controls supposed to be mediated by intracortical inhibition in V1 to be suppressive modulation, which is again inconsistent with the result of blockade of intracortical inhibition in V1 (Ozeki et al. 2004).

2.1.6. Functional roles of surround modulation

Surround suppression could be a way to encode the global structures of visual field that extends beyond the CRF or the geometrical relationships between the objects within the CRF and the surrounding field.

At single cell level, the surround suppression in V1, similar with other suppressive phenomena observed in V1 such as cross-ordination suppression, are explained by a response gain control property. Each neuron has accelerating response nonlinearity while its response divisively inhibited by a pool of broadly stimulus-tuned responses of other neurons. This gain control property optimizes the tuning performance of the processing system so as to match to the condition and configuration of stimuli in the environments. Several studies show that surround suppression, which has broadly tuned selectivity for stimulus, makes tuning properties of neural an activity of a single neuron sharper (Chen et al., 2005; Xing et a., 2005). At neuronal population level, surround suppression improves efficiency of visual information processing. Vinje and Gallant (2002) showed that, during simulated natural vision in behaving macaques, a simulation of ECRF increased the selectivity of individual V1 neurons. From the results, they

demonstrated that the surround suppression affects on the representation and transmission of information in V1 neurons because surround suppression reduces the overlap in tuning function of individual neurons. Schwarts and Simoncelli (2001) also demonstrated that nonlinearity of V1 neurons, including surround suppression, could eliminate correlations of spike response of neighboring neurons. These data suggest surround modulation in V1 take advantage of reducing the redundancy of spiking neurons and of encoding meaningful visual information for us.

2.1.7. The aim of this study

Previous studies characterized mainly the spatial profile, such as orientation tuning and spatial frequency tuning, of surround suppression of V1 neurons by using drifting sinusoidal grating, and suggested that surround suppression is profitable in reducing the redundancy of spatial structure and in encoding the global structures of visual field. This scheme alone, however, is not sufficient to evaluate the property and functions of surround suppression. Our visual functions are depending not only on the spatial context, but also on the temporal context. To evaluate the functional role of surround suppression in V1 neurons, it is indispensable to characterize the temporal profile of surround suppression. Therefore, in this study, I characterized the temporal profile of surround suppression with a stationary sinusoidal grating. A stationary sinusoidal grating is suitable stimulus for this purpose and was used in previous studies, which focused on time course of neural responses.

The goal of this study is to characterize the temporal profile of surround suppression in V1, and to investigate functional role of surround suppression. For the purpose, first, I examined the temporal profile of spatial frequency tuning curve of surround suppression of V1 neurons by using stationary flashes of sinusoidal grating as visual stimuli. Second, I examined the

difference in spatial and temporal profile between surround suppression and CRF response. Not only understanding the functional difference in the temporal aspect between surround suppression and CRF response, but also investigating their neural mechanisms, it is essential to compare these with a particular focus on the spatial frequency tuning.

2.2. Methods

2.2.1. Materials

All efforts were made to minimize animal suffering and to reduce the number of animals used. All procedures were performed in accordance with confirmed to those established by the National Institute of Health Guidelines for the Care and Use of Laboratory Animals (1996) and the guidelines of the Animal Care Committee of the Osaka University Medical School.

2.2.2. Preparation

Ten adult cats weighing 2-3.5kg were used in this study. Dexamethasone (Decadron-A, Banyu Pharm., Tokyo) was injected (0.1 mg ,i.m) 24-36 h before the start of the experiments. Atropine (0.02 mg/kg, i.m.) were injected 20 min before surgery. Animals were anesthetized with ketamine (5 mg/kg, i.m.) followed by a mixture of isoflurane (1-3%) and N₂O:O₂ (2:1). The trachea of each animal was incubated, and a catheter was placed in the femoral vein. The animals were then placed in a stereotaxic head holder, continuously paralyzed with pancuronium bromide (0.1mg/kg/hr, i.v.) to minimize eye movements and maintained under artificial ventilation. During the recording of neuronal activity, isoflurane was reduced to 0.3–1.0 % in N₂O:O₂ (2:1), and fentanyl citrate (Fentanest; Sankyo, Tokyo, Japan; 10 µg/kg/hr, i.v.) was continuously infused. The eyes were refracted using O₂-permeable contact lenses to be focused on a CRT display. The rectal temperature was maintained at 37-38 °C with a thermostatically controlled heating pad. The EEG and ECG were continuously monitored

throughout the experiments.

2.2.3. Physiological recording and visual stimulation

Tungsten in glass microelectrodes (Levick, 1972) was used for extracellular single-unit recordings. When neurons were encountered, a single unit activity was isolated on the basis of its spike waveform and magnitude with Multi Spike Detector (Alpha Omega Engineering, Israel) and stored at a resolution of 0.1 ms.

Before the main tests for temporal analysis of surround suppression and CRF response using stationary grating, three types of preliminary characterization of RF using stationary flashed bar, drifting and stationary gratings were performed as follows. The minimum response field (Barlow et al., 1967) was manually plotted on a tangent screen placed 57 cm in front of the eyes of the cats, and its basic response properties, such as dominant eye, optimal orientation and direction of stimulus, SF, ON/OFF characteristics with respect to a stationary flashed bar, and tuning to stimulus length and velocity were assessed with a hand-held projector to promote the accurate centering of the minimum response field.

Next, the computer-generated visual stimulus was targeted to the center of the minimum responsive field. The sinusoidal grating was generated by a stimulus generator (VSG2/3; Cambridge Research Systems, Rochester, UK) and was presented monocularly on a display (CPD-G500J, SONY; mean luminance 30 cd/m²; screen size, 40 x 30 cm²; resolution, 1024 x 768 pixels; and refresh rate, 100 Hz), which was placed 57 cm in front of the animal's eyes. Nonlinearities in phosphor output were corrected by lookup tables.

The parameters of grating (orientation, SF, spatial phase, temporal frequency (TF), contrast, and size (diameter of circular grating patch)) were controlled independently. Using

drifting grating followed by stationary grating, where the neuronal responses to the gratings were quantitatively and systematically measured as a function of each parameter, carried out the quantitative measurements of CRF properties. Spike responses were accumulated as raster display, peristimulus-time histogram (PSTH), and response-tuning curve along a given dimension on-line, and the optimal parameters were determined on the basis of total number of spikes evoked for CRF stimulation period. The CRF size was determined by expanding the radius of circular patch of an optimal grating until the neuron's response stopped increasing (Cavanaugh et al., 2002) at stimulus contrast eliciting subsaturating responses (80-90 % of maximal response).

The drifting grating was presented for 2 sec in a random sequence for each dimension of parameters, and each stimulus presentation was interleaved for 2-4 sec with a blank screen with the same mean luminance (30 cd/m^2) as the stimulus gratings. According to the responses to drifting grating with optimal parameters, neurons were classified into either simple or complex cells on the basis of F1/F0 ratio (Skottoum et al., 1991, see "Data analysis" section).

Subsequently, CRF characterization was done using stationary grating. The grating was turned on for 500 ms in a random sequence for each dimension and then turned off for 2-4 sec. The optimal parameters were determined by constructing response-tuning curves for individual parameters including spatial phase using the same protocols as drifting grating.

Following the preliminary CRF measurements, we performed two types of main tests to examine the effects of SF of stationary ECRF and CRF gratings on surround suppression and CRF response, respectively. (1) The optimal grating was presented within the CRF for 500 ms alone or in conjunction with the annular (ECRF) grating abutting to the CRF, which was flashed for 50 ms. The SF of the ECRF grating was varied ranging 0.1 to 1.6 c/deg; SF difference, -3 $-$ $+3$ in octave while the other stimulus parameters were kept identical to the CRF grating (SF

tuning test of surround suppression). (2) The CRF was stimulated in the absence of ECRF grating. The SF of the CRF grating was varied (0.1 –1.0 c/deg), but other parameters were fixed at the optimal for the neuron (SF tuning test of CRF response). To estimate the SF bandwidth accurately in both tests, the transitions of SF tuning curve were carefully examined.

2.2.4. Data analysis

For each neuron, the fundamental (F0) and first harmonic (F1) components of the average response were computed from PSTHs that were compiled during the characterization of the RFs. Cell type was classified into either simple or complex on the basis of the F1/F0 ratio (F1/ F0 >1, simple cell; F1/F0 < 1, complex cell).

Analysis of response latency

PSTHs were filtered in time with a Gaussian of an SD of 2 ms and plotted in units of spikes per second. Response latency was computed as the time when the difference in magnitude between reference response and test response became 5% of the maximum difference (Bair et al. 2003). For the latency of surround suppression, the reference was the response to the CRF stimulus alone, and for the test of SF tuning of CRF response, the reference was the firing of trial of 500 ms without stimulus.

Spatial frequency (SF) tuning

To know the temporal characteristic of SF tuning, we calculated SF tuning curves at four different time windows of response, 0–500 ms, (total response), 0–50 ms, 50–100 ms and 100–150 ms. In the CRF-SF tuning test, to quantitatively describe the tuning curves, the data

were fitted with the following function:

$$R(sf) = K_e * e^{-(sf-SF_e)^2/2\sigma_e^2} + K_i * e^{-(sf-SF_i)^2/2\sigma_i^2}$$

$R(sf)$ is the response, and sf , K_e , K_i , SF_e , SF_i , σ_e , and σ_i are the spatial frequency, amplitudes, means and widths of two Gaussian functions. SF_e , SF_i , K_e , K_i , σ_e and σ_i were optimized to provide the least squared error fit to the data, using MATLAB FMINSEARCH.

In the SF tuning test of surround suppression, the data were fitted with the following function:

$$SI(sf) = K * e^{-(sf-SF_{peak})^2/2\sigma^2} + Ro$$

Suppression index (SI) is the strength of the maximal surround suppression normalized by the activity, and the index takes a value between 0 (no suppression) and 1 (complete suppression). K is the amplitude of suppression and SF_{peak} and σ are the mean and width of Gaussian and Ro is base line of suppression. Values of K , σ , Ro and SF_{peak} were optimized to provide the least squared error fit to the data, using MATLAB FMINSEARCH.

In both SF tuning tests, we then calculated four indices from fitting data, the peak of SF (SF_{peak}), high-cutoff SF (SF_{high}), SF width (SF_{width}) and low SF suppression ratio (LSFS). SF_{peak} is the SF, which caused the maximal CRF response or the strongest surround suppression. SF_{high} is high-cutoff SF that caused half amplitude in high SF area. SF_{width} is the SF-selectivity (sharpness of SF tuning) of the surround suppression in high SF area, which is calculated as follows:

$$SF_{width} = \log_2(SF_{high} / SF_{peak})$$

LSFS of surround suppression was defined as the ratio of SIs obtained for ECRF gratings with the lowest SF used SFs, which is typically 0.1 c/deg, ($SI(SF_{lowest})$) to the largest SI ($SI(SF_{largest})$), and LSFS of CRF response was also defined as the ratio of responses between

response with lowest SF used SFs ($R(SF_{lowest})$) and the largest response ($R(SF_{largest})$). These are calculated as follows:

$$LSFS = SI(SF_{lowest}) / SI(SF_{largest}) \text{ or } LSFS = R(SF_{lowest}) / R(SF_{largest}).$$

Calculation of LSFS uses only two points, and then the LSFS index shows a floor effect (Xing et al., 2004), but it could be calculated even when we could not fit the curve and therefore we used this index.

Data from some neurons could not be fitted with Gaussian function because of small number of data points and occasional response increase etc. In such a case, SF_{peak} was taken as SF to cause the strongest suppression in raw data without fitting, but those data were excluded from analysis of SF_{high} and SF_{width} .

2.3. Results

In order to understand the spatiotemporal nature of cortical processing of visual information given in the classical receptive field (CRF) and in the extraclassical receptive field (ECRF), we examined time course of CRF response and ECRF-induced surround suppression with a particular focus on the spatial frequency (SF) of stimuli. A total of 120 neurons were stably recorded for more than three hours. The neurons were classified into simple cells and complex cells on the basis of the F1/F0 ratio of visual responses to drifting sinusoidal grating stimulus (see Materials and Methods).

2.3.1. Spatiotemporal properties of Surround suppression

To explore the spatiotemporal property of ECRF underlying surround suppression, the temporal

dynamics of surround suppression and its dependency on SF of ECRF stimulus were examined. The stationary sinusoidal grating patch (CRF stimulus) and the annulus (ECRF stimulus) were concurrently flashed to CRF for 500 ms and to ECRF for 50 ms, respectively. We analyzed 51 neurons that exhibited more than 20 % reduction of CRF response by the ECRF stimulation in, at least, one of stimulus conditions tested.

Stimulation of ECRF reduced the CRF response, and not only the strength but also the time course of surround suppression varied depending on SF difference between ECRF stimulus and CRF stimulus (**Fig 2.A-G**). **Figure 2** shows an example of PSTHs obtained from a single neuron in V1. Each curve indicates the response averaged over 30 trials of each stimulus condition. The thick and thin lines show the responses to the CRF stimulation with and without ECRF stimulus, respectively. This cell exhibited a strong phasic response followed by weak sustained response to the CRF stimulation with optimal parameters of sinusoidal grating patch (diameter, 5 deg; SF, 0.3 c/deg) (**Fig 2.A-G**, thin lines). The ECRF stimulation (20 deg in diameter) with 7 different SFs (0.1 – 0.9 c/deg) caused different amounts of reduction in spiking rate, ranging from 11% to 50%. The strength of the surround suppression was quantitatively assessed as suppression index (SI) calculated with total number of spikes evoked during CRF stimulation with or without ECRF stimulation (shown at the top-right of each PSTH). The strongest suppression was yielded when ECRF and CRF was stimulated with the same SF (SF = 0.3 c/deg, SI = 0.50) and the magnitude of SI decreased as the SF difference increased, corresponding to the results of previous studies (DeAngelis et al., 1994; Li and Li, 1994). The dependency of surround suppression on the SF difference between CRF and ECRF is conspicuous in the temporal profiles of PSTHs (**Fig. 2 A-G**). That is, onset latency of the surround suppression was delayed as the SF of ECRF stimuli increased. ECRF stimulus with the lowest SF (0.1 c/deg) induced a rapid suppression, by which even the earliest part of CRF

response was suppressed completely. When the SF of ECRF-stimuli was equal to or larger than 0.2 c/deg, the onset of the suppressive effect was later than that of the excitatory response to CRF stimulation.

To quantify the SF dependency on temporal properties of surround suppression in detail, two measures, the onset latency of suppression (suppression latency) and temporal characteristics of SF tuning in suppression. First, we calculated the suppression latency as the time point when the magnitude of response to the combined stimulation of CRF and ECRF deviated from that of the response to CRF stimulation by 5 % of the maximum difference (see Materials and Methods). The temporal analysis demonstrated that the shortest suppression latency was observed for ECRF stimulus with lowest SF (0.1 c/deg: 29 ms), and it increased from 29 ms to 46 ms with the increase in the SF of ECRF stimulus (**Fig2. A-G**, latency is shown at the top-right of each PSTH). The relationship of SFs to ECRF stimulation for the suppression latency is shown in **Fig. 3**, where the suppression latencies measured for responses at the lowest SF condition with SI larger than 0.2 were plotted against those at condition of SF optimal for CRF response. Most of data points fell above the diagonal line. The suppression latency at low SF was significantly shorter than that at optimal SF (paired t-test; $p < 0.05$), and the mean difference was 9.82 ms. Thus, the ECRF stimuli with low SF induced the rapid suppression regardless of the average strength of suppression by ECRF stimulation with the optimal SF.

——— Response for classical receptive field
 ——— Response for classical receptive field and extraclassical receptive field

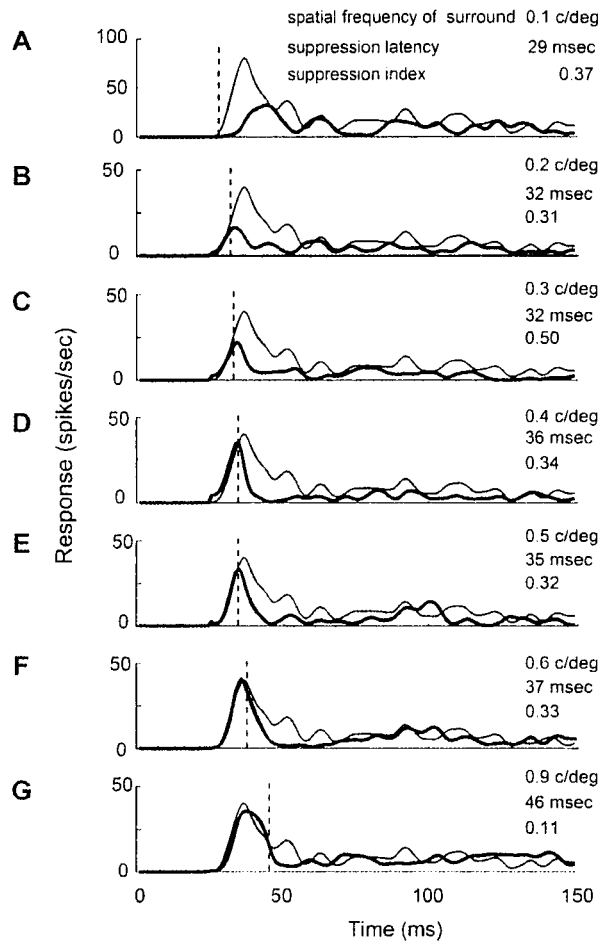


Figure 2

SF selectivity of surround suppression in V1 neuron (A–G). Spike response traces recorded with presentation a grating patch, which is classical receptive field (CRF) stimuli (spatial frequency = 0.3 c/deg), with (thick line) and without (thin line) grating annulus (“ECRF stimuli”). Spatial frequency of ECRF stimuli, suppression index, and suppression latency (dashed line) are shown at the top-right of each PSTH.

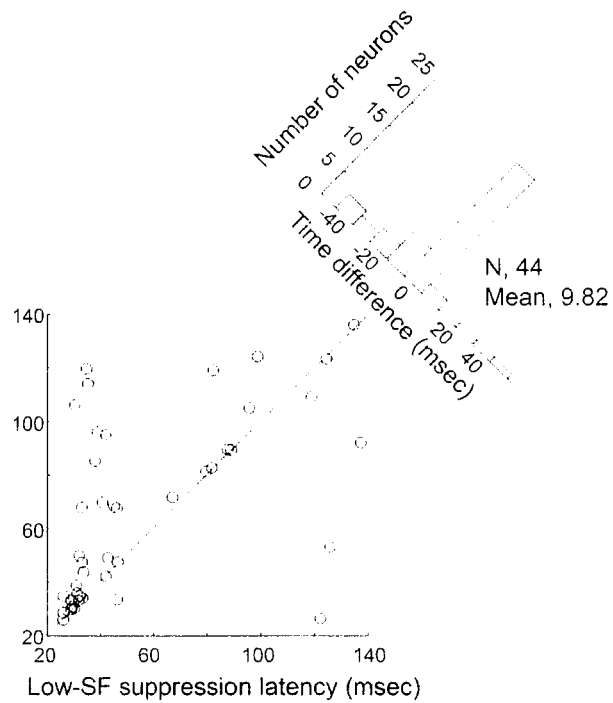


Figure 3

Comparison of onset latency of surround suppression with optimal spatial frequency and that with lowest spatial frequency that evoked suppression for individual V1 neurons.

Onset latency for surround suppression with preferred spatial frequency is against onset latency with lowest spatial frequency, which evoked strength of surround suppression larger than 0.2.

For the 44 neurons, the difference of onset latency by increment of spatial frequency of surround annulus was 9.82 ms.

2.3.2. Temporal characteristics of SF tuning in surround suppression

In most of neurons, CRF response was reliably observed for the first 150 ms after the stimulus onset. Accordingly, the surround suppression was also reliably observed during that period, which is suitable to precisely analyze temporal properties of surround suppression. Therefore, I divided the response into three time windows and constructed the SF-tuning curves of SI from those windows in addition to whole response period of 500 ms (**A**, Full window (0–500 ms), **B**, first window (0–50 ms), **C**, second window (50–100 ms), **D**, third window (100– 50 ms)).

Figure 4 shows the tuning curves of SI plotted against SF of ECRF grating for responses of a neuron depicted in **Fig. 2**. The CRF was constantly stimulated with grating of optimal parameters. The SF of CRF grating was 0.3 c/deg (dashed vertical lines in figures). The SF tuning properties of surround suppression dramatically changed during the first 150 ms after the stimulus onset. The tuning curve showed low-pass type of SF tuning at the first window (**Fig.4B**), and the peak SF of tuning curve was lower than 0.05 c/deg. Therefore, the SF tuning curves become band-pass shape with the peak around 0.3 c/deg, which is same as the SF of CRF stimulus (**Fig. 4C and D**). To analyze the shift of SF tuning quantitatively in our sample population, next we measured peak SF (the most effective SF of ECRF grating) for surround suppression.

The histograms of the most suppressive SF difference between CRF and ECRF gratings are shown in **Figure 5** for the four time windows. We first studied SF preference of surround suppression of total response calculated from total number of spikes evoked during CRF stimulation (0–500 ms) (**Fig. 5A**). The histogram was peaked at the SF difference 0 and most of neurons fell within ± 1 octaves, suggesting that CRF response is maximally suppressed

when SF of ECRF grating is same as or similar to the optimal SF of CRF grating (mean \pm sd, -0.28 ± 1.63 in octave). This result is consistent with the previous findings obtained by drifting sinusoidal grating (DeAngelis et al., 1994; Li and Li, 1994).

Figure 5B, C, and D show results obtained from each 50 ms time window (**B**, first window (0–50 ms), **C**, second window (50–100 ms), **D**, third window (100–150 ms)), where eight neurons were excluded from this analysis because of unstable CRF responses for the first 150 ms after stimulus onset. At the first window (**Fig. 5B**), about 60 % of neurons ($n = 29$ of 46) were maximally suppressed by ECRF-stimuli with SF lower than that of the CRF-stimuli (mean \pm sd; -1.20 ± 1.95 in octave). Therefore, the distribution shifted to close to SF difference = 0 at the second and third windows (mean \pm sd; second window, -0.42 ± 1.85 ; third window, 0.08 ± 1.21 in octave). The difference between first and third windows was statistically significant ($p < 0.05$; ANOVA followed by LSD post hoc test). Thus, the most effective SF of surround suppression dynamically shifts along response time course from low SF to the same SF as CRF (the optimal SF for CRF of the neuron). The shift of peak SF is attributable to a decrease of suppressive effect at low SF of ECRF grating or an increase at high SF, or both of them. To examine how the SF-tuning curve for surround suppression temporally changes in detail, we analyzed four parameters to characterize SF-tuning curve of SI shown in **Fig. 4** as an example: peak SF (SF_{peak}), high cutoff SF (SF_{high}), width between SF_{peak} and SF_{high} (SF_{width}) and low spatial frequency suppression ratio (LSFS); (Ringach et al., 2002a; Xing et al., 2004). Those parameters were compared between the first window and the third window (**Fig. 6**).

Figure 6A demonstrates the distribution of absolute values of SF_{peak} compared between first and third windows. Majority of data points fell above the diagonal line, and SF_{peak} for first window (abscissa; mean \pm sd; 0.27 ± 0.23 c/deg) was significantly lower than that for third window (ordinate; mean \pm sd, 0.42 ± 0.33 c/deg (paired t-test; $p < 0.05$). To quantify this

temporal change, we calculated the difference of SF_{peak} between the two time windows (**Fig. 6A-2**). The average difference in SF_{peak} was 0.89 in octaves (**Fig. 6A-2**). Thus, the SF preference for surround suppression dynamically shifted from low to high within 150 ms after stimulus onset.

As showed as an example neuron in **Fig. 4**, the SF tuning of surround suppression shifted from the low-pass type to the band-pass type along the time course of response during 150 ms after stimulus onset. To examine this point quantitatively in population, we fitted SI - SF tuning curves of raw data with the Gaussian function, and estimated effective range of surround suppression in high and low SF spectrum. Some neurons ($n = 15$) whose SI - SF tuning curves could not be reliable fitted with function were excluded from this analysis.

In a scatter diagram of high cutoff SF (SF_{high})(**Fig. 6B-1**), 67 % of neurons ($n = 17$ of 27) fell above the diagonal line. The mean difference between two time windows was 0.52 in octaves, which was statistically significant (paired t-test; $p < 0.05$) (**Fig. 6B-2**). Thus, SF_{high} as well as SF_{peak} shifted toward high SF along time course of response. Therefore, it didn't cause significant change in the tuning width in high SF area (SF_{width}) in our sample population. Scatter diagram for SF_{width} showed the distribution of data points unbiased to the diagonal line (**Fig. 6C-1**), and histogram exhibited a distribution centered at difference = 0 between two time windows (mean difference, -0.75 octave; paired t-test, $p = 0.09$) (**Fig. 6C-2**). However, it should be noted that a certain population of neurons deviated far from the diagonal line and fell on near abscissa of scatter plot (**Fig. 6C-1**), suggesting a sharpening (narrowing) the tuning to temporal change of SF_{width} varies from neuron to neuron. Last, temporal change of SF tuning of surround suppression particularly at low SF range was examined as change of low SF suppression ratio (LSFS) (**Fig. 6D**). In the first window (abscissa); the mean value of LSFS was 0.69 ± 0.48 and approximately 60 % of neurons ($n = 25$ of 42) took value of 1, suggesting that the ECRF grating

with the lowest SF was effective at early phase of surround suppression. At later phase, the suppressive effect of lowest SF stimulation attenuated rapidly, and the LSFS decreased to 0.25 ± 0.69 in the third window. The difference between mean values of those windows was significant (0.45 ± 0.45 , paired Wilcoxon test; $p < 0.05$). Thus, the suppressive effect induced by ECRF stimulation with low SF grating is fast and transient.

These data suggest that the SF tuning property of surround suppression dynamically changes through time along time course of response, that is, the SF tuning at the early suppression exhibits low-pass tuning, and afterward shifts to band-pass tuning that tunes close to the optimal SF of CRF response.

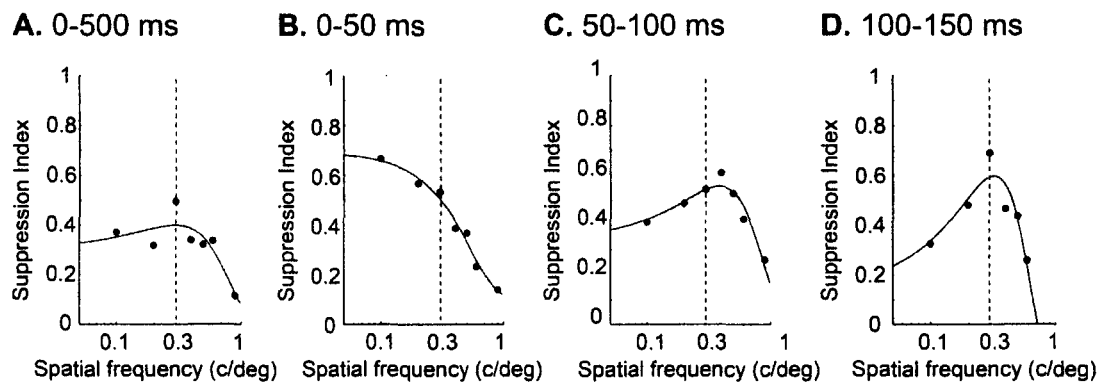
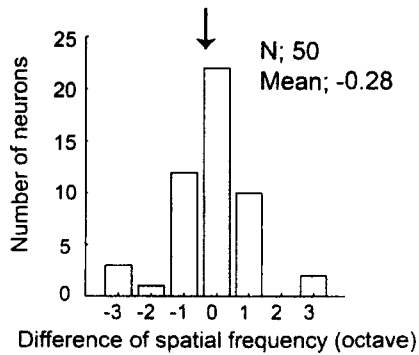


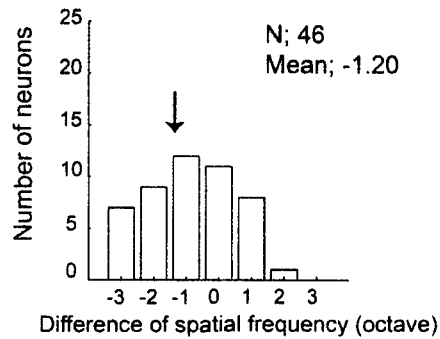
Figure 4

Temporal change of spatial frequency tuning of surround suppression. Data shows the strength of suppression at full time window of presenting stimulation (**A**, 0 –500 ms) and short time window (**B**, 0-50 ms, **C**, 50–100 ms; **D**, 100-150 ms) for the cell seen in Figs.2, as a function of annulus spatial frequency for seven-annulus spatial frequency between 0.1 and 1 c/deg. Curves are fits with a simple descriptive function (see Materials and methods). Preferred spatial frequency of surround suppression change along the time after stimulus onset (**B**, **C**, **D**)

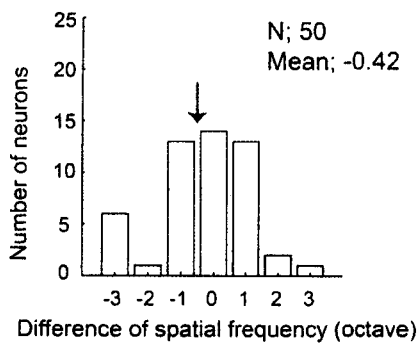
A. 0-500 ms



B. 0-50 ms



C. 50-100 ms



D. 100-150 ms

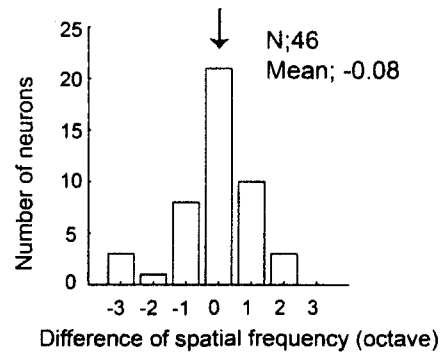


Figure 5

Distribution of relative spatial frequency between CRF stimuli and most effective spatial frequency of surround stimuli. Strength of surround suppression were measured from mean firing rate during 0–500 ms (**A**) and during short time windows (**B**, 0–50 ms, **C**, 50–100 ms and **D**, 100–150 ms) in response to stationary grating. The relative spatial frequency was calculated as the ratio of spatial frequency in octaves (see Material and methods).

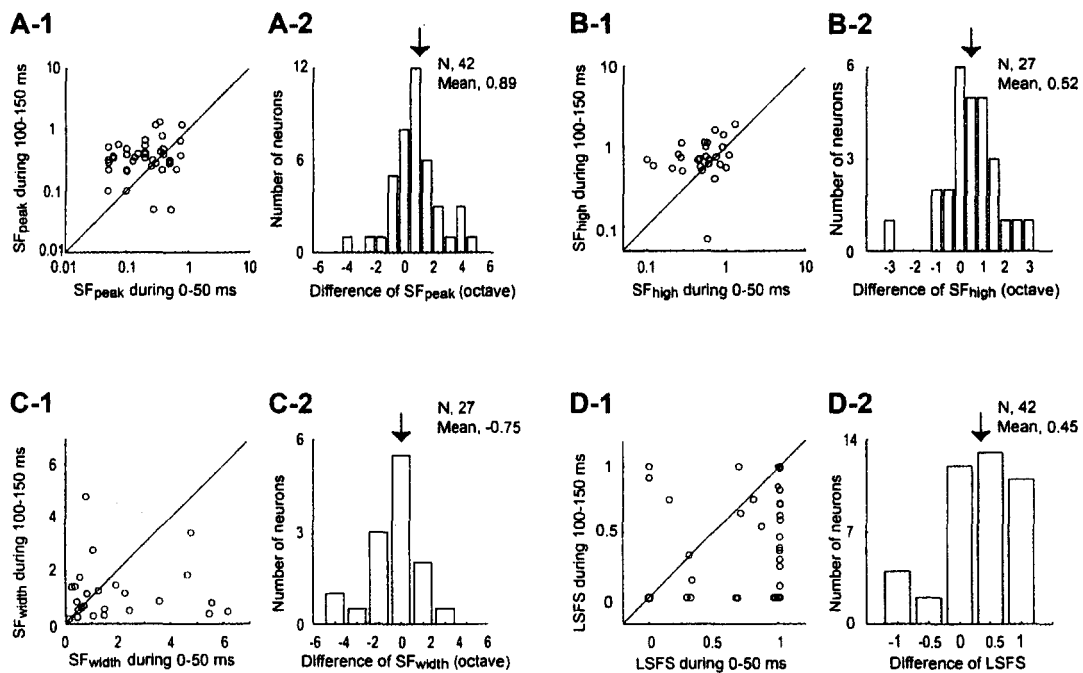


Figure 6

Summary of the temporal shift of SF tuning of surround suppression in population. Panels illustrated four key parameter of SF tuning, peak spatial frequency (SF_{peak}), high out off spatial frequency (SF_{high}), width of spatial frequency tuning (SF_{width}), and low spatial frequency suppression ratio (LSFS). Points that lie above and below the diagonal indicated and increase or decrease in the parameter value along time. (A-1) The SF_{peak} at early time window (0–50 ms) plotted against the SF_{peak} at late time window (100–150 ms). (B-1, C-1, D-1) Same as A-1, the SF_{high} , SF_{width} , and LSFS at early time window plotted again those at late time window. (A-2, B-2, C-2, D-2) Distribution of difference between SF_{peak} (A-2), SF_{high} (B-2), SF_{width} (C-2) and LSFS (D-2) at early time window and those at late time window. Arrows indicate mean values of the distributions.

2.3.3. Temporal characteristics of SF tuning in CRF response

There are studies reporting that, SF-tuning of CRF response of V1 neurons shifted from low to high with time (Bredfeldt and Ringach, 2002; Mazer et al., 2002; Frazor et al., 2004). If such a property of CRF response is responsible for the temporal shift of SF tuning of surround suppression observed in the present study, there is a possibility that both phenomena share a common temporal property of SF tuning. In order to examine this point, we analyzed the temporal property of SF tuning of response to CRF stimulation.

Figure 7 shows the PSTHs for the CRF responses to stationary sinusoidal grating patch of optimal parameters with varying SFs (0.1-1 c/deg). Each curve indicates the response averaged over all trials (25 trials). The neuron responded best to the grating with SF of 0.5 c/deg, causing the distinct phasic response followed by the weak sustained response. It tuned to a narrow range of SF, and neither low SF (such as 0.1-0.2 c/deg) nor high SF (1 c/deg) grating evoked any response, indicating a band-pass SF tuning. The dashed vertical lines indicate the onset of CRF responses. The onset latency was progressively prolonged from 28 ms to 52 ms as SF of grating patch was increased. The marked delay observed for response to high SF grating (0.9 c/deg) (**Fig. 7G**) might be simply due to weakness of response. The SF-dependency of onset latency for surround suppression was characterized as a faster onset of suppression at low SF grating comparing to that at optimal SF grating. To quantitatively examine whether the CRF response shows similar property, next, we compared the onset latency of responses to CRF stimulations with optimal SF and that with lowest SF (**Figure 8B**).

Figure 8B demonstrates a scatter diagram of onset latency of CRF responses with low and optimal SFs. Most of data scattered around the diagonal line only with only a slight bias below the diagonal. The histogram of time difference depicted in upper right of **Fig.8B** seems

like a mirror image of that for surround suppression (**Fig. 3**), suggesting that onset latency of response to optimal SF stimulation is not significantly delayed to that of response to low SF stimulation. Thus, onset latency of CRF response changed depending on SF of CRF grating in some neurons, but the amplitude of change is substantially smaller than that observed in surround suppression.

Temporal dynamics of the SF tuning of CRF response was also different from that of surround suppression. The SF tuning curves of CRF response of the same neuron shown in **Fig.7** were constructed for four different time windows (**Fig. 9: A**, Full window (0–500 ms), **B**, first window (0–50 ms), **C**, second window (50–100 ms), and **D**, third window (100–150 ms)). The peak of tuning curves (SF_{peak}) tended to shift from low SF to high SF with time (Full window, 0.54 c/deg; first window, 0.43 c/deg; second window, 0.56 c/deg; third window, 0.61 c/deg), but the change was very small (0.18 c/deg). The most prominent difference in comparison with surround suppression was that the band-pass SF tuning of the CRF response was remained regardless of window.

To quantify the temporal change of SF tuning of CRF response, we calculated peak of tuning curve (SF_{peak}), tuning width (SF_{width}), SF eliciting the half-maximal response (SF_{high}) and low spatial frequency suppression ratio (LSFS) (see Materials and Methods), and compared between first window and third window. Ten neurons out of seventy-two were excluded from the following analyses, since sufficient response was not obtained from either first or third window.

In the scatter diagram of peak SF (**Fig.10A-1**), sixty-five percent of neurons ($n = 39$ of 62) fell above the diagonal line, indicating the temporal shift toward high SF. The mean difference between two time windows was 0.27 ± 0.84 in octaves (**Fig. 10A-2**), which was statistically significant (paired t-test; $p < 0.05$). Thus, the temporal change in peak SF from low

to high is a common property between CRF response and surround suppression, but the strength of shift is smaller for CRF response comparing with 0.89 octaves for surround suppression (**Fig. 6A-2**).

In contrast to the case of surround suppression, the shift of peak SF was not accompanied by the shift of high cutoff SF (SF_{high}). In the scatter graph (**Fig. 10B-1**), data points distributed near the diagonal line with a little bias toward upper side, but no significant difference was observed between two time windows (**Fig. 10B-2**; paired t-test, $p = 0.06$). Also, SF bandwidth showed temporal change without noticeable bias to particular direction (**Fig. 10C**). In **Fig.10C-1**, data points were widely scattered and there was no significant difference between two time windows (paired t-test; $p = 0.26$). Thus, the change of SF bandwidth varied from neuron to neuron. In **Fig.10D-1**, I compared the temporal change of SF tuning at low SF range. In contrast to the case of surround suppression, at early time window, mean value of LSFS was 0.34 and only about 10% neurons ($n = 8$ of 62) took value of LSFS 1, and this trend did not shift with time (0–50 ms, 0.34 ± 0.34 ; 100–150 ms, 0.32 ± 0.34 , paired t-test, $p = 0.6$ and **Fig. 10D-2**).

These data suggest that the SF selectivity of CRF response changed along time after the stimulus onset, and that peak SF of tuning curve slightly shifted from low to high SF. But tuning curve was consistently band-pass type through all response time windows. In contrast to the tuning curve of surround suppression, low SFs around 0.1 – 0.2 c/deg are not effective SF for CRF response.

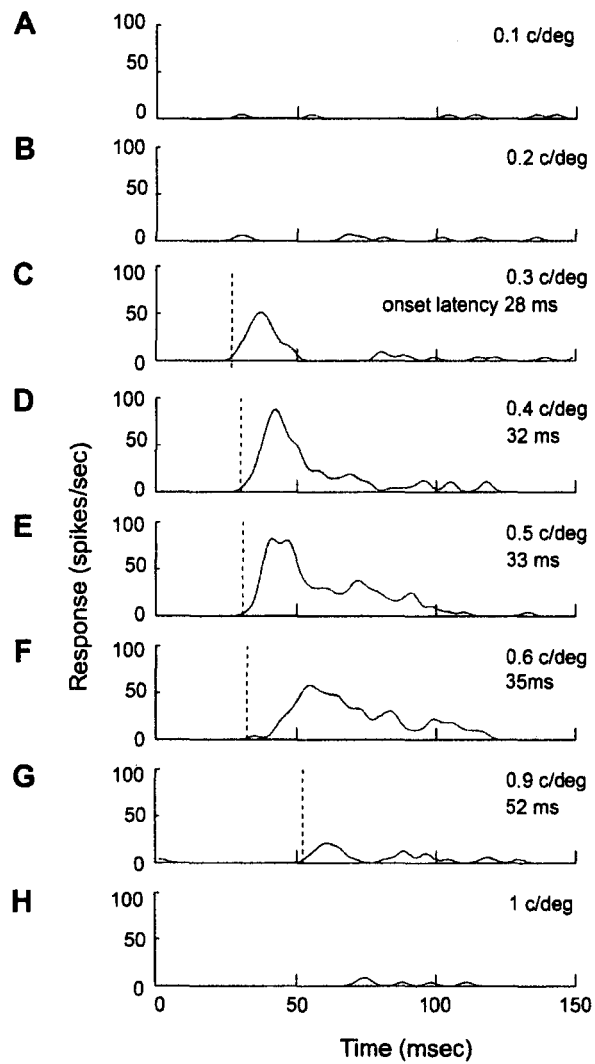


Figure 7

SF selectivity of response to classical receptive field stimulation. Spike response traces recorded with presentation a grating patch with optimal size (“classical receptive field stimuli (CRF stimuli)”), varying spatial frequency (SF) from 0.1 c/deg to 1 c/deg. SF of CRF stimuli. SF of CRF stimuli and onset latency (dashed line) are shown at the top-right of each PSTH.

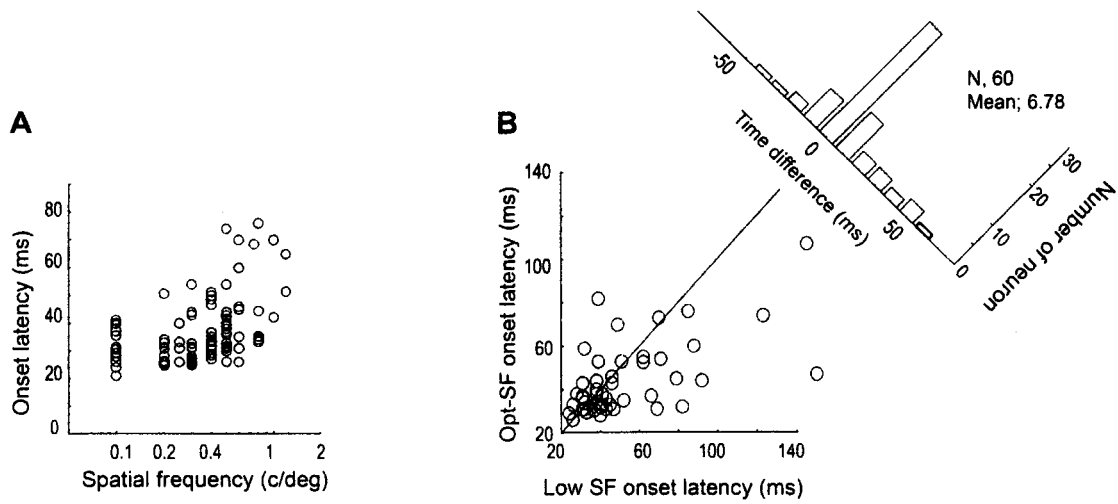


Figure 8

Relationship between onset latency and spatial frequency. (A) Onset latency for response to classical receptive field (CRF) stimulation with optima spatial frequency (SF) is plotted against that that optimal SF. Positive correlation was observe between SF and onset latency. (B) Comparison of onset latency between with optimal spatial frequency and lowest SF. Onset latency for response to CRF stimulation with preferred SF against onset latency with lowest spatial frequency, which evoked significant spike response.

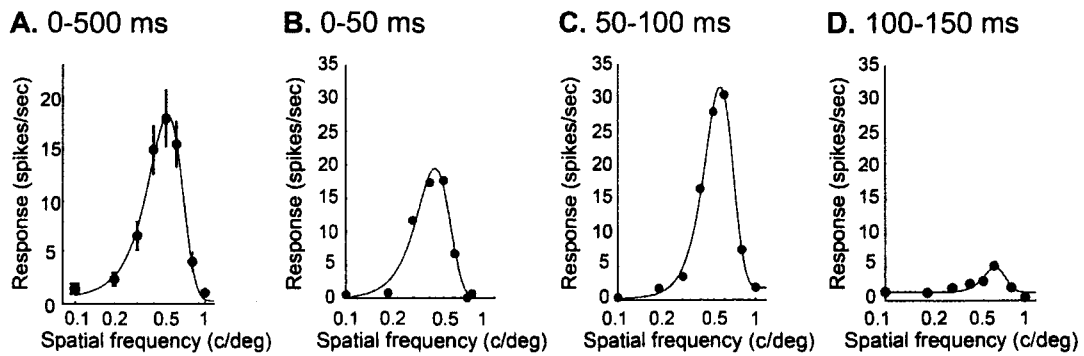


Figure 9

Temporal change of spatial frequency tuning of response to classical receptive field stimulation. Data shows the mean firing rate responses of as a function of spatial frequency at full time for stimulus presentation (A, 0-500 ms) and at short time window (B, 0-50 ms, C, 50–100 ms; D, 100-150 ms) for the cell seen in Figs.7. Curves are fits with a simple descriptive function (see Materials and methods).

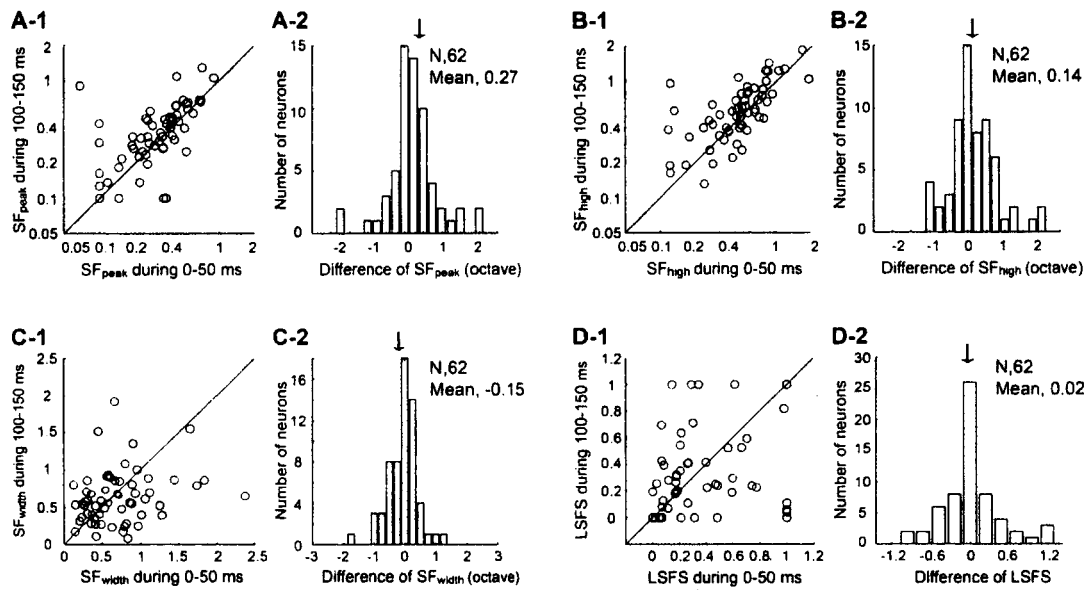


Figure 10

Summary of the temporal shift of SF tuning of response to CRF stimulation in population.

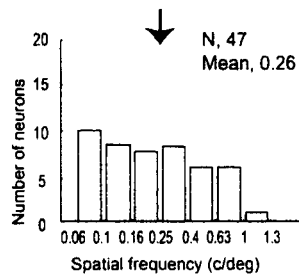
Panels illustrated four key parameter of SF tuning, peak spatial frequency (SF_{peak}), high off spatial frequency (SF_{high}), width of SF tuning (SF_{width}), and low spatial frequency suppression (LSFS). Points that lie above and below the diagonal indicated and increase or decrease in the parameter value along time. (A-1) The SF_{peak} at early time window (0–50 ms) plotted against the SF_{peak} at late time window (100–150 ms). (B-1, C-1, D-1) Same as A, the SF_{high} , SF_{width} , and LSFS at early time window plotted again those at late time window. (A-2, B-2, C-2, D-2) Distribution of difference between SF_{peak} (A-2), SF_{high} (B-2), SF_{width} (C-2) and LSFS (D-2) at early time window and those at late time window.

2.3.4. Comparison of tuning in CRF-response and surround suppression in V1

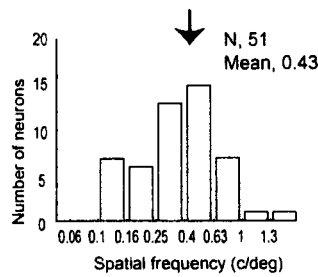
The most effective SF for surround suppression showed considerable shift from low to high values along the time course of the response comparing to that for CRF response, suggesting contributions of plural mechanisms with different SF tuning. In order to obtain a clue for understanding the neuronal mechanism on this point, I should know when and how much the SF tuning is associated or dissociated between surround suppression and CRF response. Especially, the dissociation suggests an involvement of visual areas other than V1 to surround suppression. Therefore, finally, I directly compared the distribution of SF preference for CRF response and for surround suppression in different time windows (**Fig. 11**). **Figure 11** shows frequency histograms for the most effective SFs against absolute SF values of ECRF grating (**Fig. 11A1-3**) and CRF grating (**Fig. 11B1-3**). The prominent difference was appeared in the distribution in the first window (**Fig. 11A1 and B1**). The histogram for surround suppression (**Fig. 11A-1**) was strongly biased toward low SF, with a peak at the lowest SF. In contrast, CRF response (**Fig. 11B-1**) showed a distribution centering around 0.3 c/deg, and only small population of neurons tuned to the extremely low SF, reflecting that most of V1 neurons have band-pass SF tuning property. Therefore, the fast surround suppression evoked with low SF grating is expected to be generated from neuronal networks having fast onset and low SF preference such as Y-pathway in subcortical level. Later than the first window, the dissociation of distributions disappeared quickly, which was mainly due to drastic rightward change in the distribution of surround suppression (**Fig. 11A-2**), while such a rightward shift was observed a bit in that of CRF response (**Fig. 11B-2**). Two distributions became even more similar in the third window (**Fig. 11A-3, B-3**). Thus, delayed surround suppression tuned to optimal SF for CRF response, suggesting an involvement of neuronal networks having band-pass SF tuning.

Surround suppression

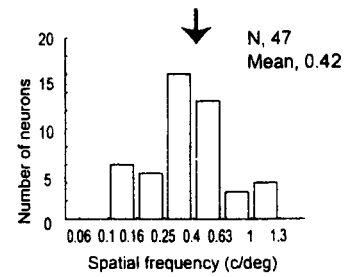
A-1. 0-50 ms



A-2. 50-100 ms

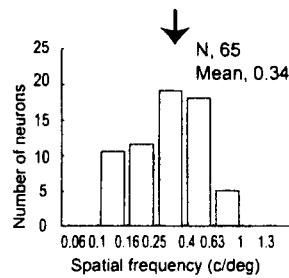


A-3. 100-150 ms

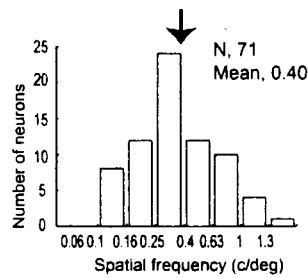


CRF response

B-1. 0-50 ms



B-2. 50-100 ms



B-3. 100-150 ms

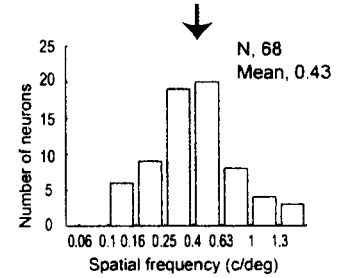


Figure 11

Distribution of preferred spatial frequency for surround suppression and response to classical receptive field stimulation. (A) (A-1) Preferred spatial frequency (SF) for surround suppression at the first (0–50 ms), (A-2) at the second (50–100 ms), and (A-3) the third time window (100–150 ms). (B) Similar measurements for response to classical receptive field (CRF) stimulation. (B-1) Preferred SF at the first time window, (B-2) at the second time window, and (B-3) at the third time window.

2.4. Discussion

I examined the temporal profiles of surround suppression and CRF response in relation to SF of ECRF and CRF grating in cat V1. I found that the time course as well as the strength of surround suppression varied depending on SF of ECRF grating. Basically, the ECRF gratings with low SF (< 0.2 c/deg.) induced a fast onset and transient suppression in comparison with the ECRF gratings with high SF (> 0.3 c/deg.). The SF tuning of surround suppression was low-pass at the early phase of the response (~ 50 ms), in which low SFs were most effective for the majority of neurons (**Figs. 4B and 5B**). Then, the effectiveness of low SFs attenuated rapidly (**Fig. 6D**) and the most effective SF shifted toward higher SF (**Fig. 6A**), resulting in band-pass characteristic of SF tuning at the later phase of response (100 – 150 ms). This is essentially due to a shift of tuning curve toward the optimal SF for CRF response (**Fig. 5D**).

The SF tuning property of CRF response also significantly changed along time (**Fig 10A**). However, the temporal shift of SF preference of CRF response was much smaller than that for surround suppression (**Fig. 11**). That is partly because the very low SF grating elicits little response for the stimulus of CRF size in most of V1 neurons and the SF tuning of CRF response remains to be band-pass throughout the response time course.

2.1. Mechanisms underlying the surround suppression

What is the origin of surround suppression in V1? At least, four possible neuronal mechanisms have been proposed: 1) Mechanisms of suppression or gain control operating at subcortical levels such as LGN (Li and He, 1987; Jones and Sillito, 1991; Ozeki et al., 2004; Sun et al.,

2004; Sadakane et al., 2006; Naito et al., 2007) or retina (McIlwain, 1966), 2) horizontal projection and intracortical inhibition in V1 (DeAngelis et al., 1994; Walker et al., 1999, 2002; Anderson et al., 2001; Sceniak et al., 2001; Angelucci et al., 2002; Cavanaugh et al., 2002a; Levitt and Lund, 2002). 3) feedback projection from V1 to LGN might modulated output of LGN (Murphy and Sillito 1996; Murphy et al., 2000; Sillito and Jones, 2002 for review), and 4) feedback projections from the extrastriate cortex (Bullier et al., 2001; Angelucci et al., 2002; Levitt and Lund, 2002; Bair et al., 2003; Schwabe et al., 2006). Even though these possibilities are not exclusive to each other, the present results provide some constraints on the sources of suppression and bridge rift among studies.

SF tuning property of surround suppression dynamically changed from low-pass tuning to band-pass tuning along time course of response to 500 ms flash of stimulus presentation. What does cause the temporal change in SF tuning of surround suppression? Previous studies (Bredfeldt and Ringach, 2002; Mazer et al., 2002; Frazor et al., 2004) reported that the SF tuning of CRF response in V1 neuron varied with the time course of responses, and our study also showed properties of CRF responses similar to the results of previous studies. Although the temporal shift of SF tuning showed the tendency similar between CRF response and surround suppression, both at single neuron level (**Figs. 5 and 7**) and at population level (**Fig. 8A**), the degree of shift in SF tuning of CRF response was weaker than that of surround suppression (**Fig. 11**). I especially emphasize the point that very low SF gratings evoked fast and transient surround suppression but little response in V1 neurons. The same dissociation for SF tuning profiles between surround suppression and CRF response was reported by Webb et al. (2005) in macaque monkey V1. This strongly suggests that the low-pass SF tuning does not originate from V1. Therefore, neural circuits based on inhibitory circuits in V1 neurons seems not to be able to explain the temporal shift of surround suppression.

Another possible mechanism is that distinct neuronal networks having different spatiotemporal properties, especially different SF preferences, are involved in surround suppression. Recently, Bonin et al. (2005) characterized surround suppressive field of LGN neurons in cats by using drifting grating, and found that the SF tuning profile was low-pass tuning and that even very low SF grating (0.01 c/deg) was effective for surround suppression. Thus, the surround suppression in V1 is probable to be inherited from LGN. On the other hand, late phase of surround suppression showed band-pass tuning with a peak at the optimal SF for CRF response (**Fig. 11 A-3, B-3**). The ECRF grating with the SF same as the optimal SF of CRF response evoked the strongest suppressive effect, which is consistent with previous studies (DeAngelis et al., 1994; Li and Li, 1994; Sengpiel et al., 1997; Walker et al., 1999; Akasaki et al., 2002). This close similarity of SF preferences suggests that the network interaction among neuronal populations, which share a common SF tuning property, is involved in surround suppression. The SF selectivity of CRF response of V1 neurons (Hubel and Wiesel, 1959, 1962) is very different from those of the retinal ganglion neurons (Rodieck and Stone, 1965) and LGN neurons (Derrington and Fuchs, 1979; So and Shapley, 1979; Kaplan and Shapley, 1982; Hicks et al., 1983; Irvin et al., 1993). Therefore, late phase of suppression would be generated at the cortical level via the intracortical connection or feedback connection. I found that suppression tuned to the SF optimal for CRF response delayed to the SF tuning of CRF excitation (**Fig. 11**). Recently, Smith et al. (2006) reported in macaque V1 that surround suppression begins later than cross-orientation suppression that is thought to be subcortical in origin (Freeman et al., 2002; Priebe and Ferster, 2006). They suggested that the synaptic delay in the cortical circuits was a reason for the onset delay of surround suppression (Smith et al., 2006). Therefore, the temporal development of surround suppression having the same SF preference as CRF response in my data is likely to reflect the poly-synaptic transmissions within the cortical circuits.

Previous studies using drifting grating reported that surround suppression is more broadly tuned than CRF response to spatiotemporal parameters such as SF and TF (DeAngelis et al., 1994, Durand et al., 2002, Ozeki et al., 2004, Webb et al., 2005). I also obtained the result consistent with this for the average response for 500 ms of CRF stimulation. Surround suppression in V1 seems to reflect the suppressive phenomena that occur at multiple (subcortical and cortical) levels, which possess different spatiotemporal properties. Webb et al. (2005) characterized the surround suppression in terms of spatiotemporal tuning, and susceptibility to contrast adaptation interocular transfer. They identified two putative sources of surround suppression, that is, LGN and V1. Consistent with this notion, we recently found that the suppressive effect of ECRF stimulation become integrating wider areas surround CRF along the time course of 200 ms after the stimulus onset (Shimegi et al., 2005, 2007). In that study, the onset latency of surround suppression become progressively shorter with and increment of ECRF stimulus.

The previous study in our laboratory clarified that a blockade of intracortical inhibition by iontophoretic administration of GABA_A receptor antagonist, bicuculline, did not significantly abolish the surround suppression in cat V1 neurons (Ozeki et al., 2004). This suggests that the primary course of surround suppression is a decrease of excitatory inputs to V1 and subsequent reduction of excitatory interaction but not due to an increase of cortical inhibition. I suppose that ECRF grating with low SF inhibits responses of LGN neurons, and higher SF ECRF grating reduces the cortical excitatory inputs.

How can the cortical excitatory inputs be reduced by a large grating stimulus? Long-range horizontal connections intrinsic to V1 and feedback connection from extrastriate cortices have been proposed as the anatomical of surround suppression. Though there are studies reporting the involvement of long-range horizontal connections in V1 and the top-down

projections from higher visual cortices (Hupe et al., 1998, 2001; Angelucci et al. 2002; Angelucci and Sainsbury 2006; for review, Angelucci and Bressloff, 2006) in surround modulation in V1, the above-mentioned observations of our laboratory on surround suppression in cat V1 prompt rebuttals to those studies. First, excitatory effects of both horizontal connections in V1 and top-down projections have to be changed into inhibitory ones via operation of intracortical inhibition in V1. The result of the blockade of intracortical inhibition, however, did not significantly affect on surround suppression. There remains a question whether there is a feasible mechanism mediating effects of the horizontal connection and top-down, feedback projections. And, second, the progressive shortening of the latency of surround suppression with an increment of stimulation in ECRF is contradictory if it has to be mediated by the horizontal connection.

I could not work out on these problems as far as working on V1 of anesthetized cat. There seems to be no simple mechanism to explain the mechanism of surround suppression in V1. Further studies, including a comparison of functional significance of above-mentioned anatomical substrates between awake- and anesthetized condition, should be required.

2.4.2. Mechanisms underlying temporal shift of SF preference in CRF response

It has been reported that SF tuning of CRF response in V1 neurons shifts through time from low SF to high SF in anesthetized monkeys (Bredfeldt and Ringach, 2002; Frazor et al., 2004), awake monkeys (Mazer et al., 2002), and anesthetized cats (Frazor et al., 2004; Nishimoto et al., 2005). In accordance with those studies, I also found the significant temporal shift of the same direction. Mainly two possible mechanisms underlying the SF dynamics in V1 have been proposed: 1) the convergent input from different types of LGN neurons such as parvocellular

and magnocellular neurons in monkey or X- and Y neurons in cat (Mazer et al., 2002; Frazor et al., 2004; Weng et al., 2005), and 2) input from a single type of LGN neurons whose SF preferences change through time from low SF to high SF (Bredfeldt and Ringach, 2002) possibly due to a temporal difference between center response and antagonistic surround response (Allen and Freeman, 2006). Some of my findings provide a clue for the problem in my sample of V1 neurons. First, there was a positive correlation for CRF response between preferred SF and the shortest response latency. This will be because that the CRF stimulus with optimal SF drives least synchronized excitatory inputs to the neurons. Second important observation on this point is that onset latency of CRF response is positively correlated with the optimal SF of neurons, that is whose optimal SF is low exhibited short response latency, where those with high optimal SF exhibited long response latency (**Fig. 8A**) The higher the cell has SF preference for CRF response, the more its onset latency is delayed. Thus, spatiotemporal property of each LGN input is conserved/reflected in CRF responses of individual V1 neurons, implying that each geniculocortical projection from distinct types of LGN neurons are separated in V1 (Ferster and LeVay, 1978; Gilbert and Wiesel, 1979) and connected to distinct population of neurons (Bullier and Henry, 1979; Ferster and Lindstrom, 1983; Tanaka, 1983; Martin and Whitteridge, 1984; Mullikin et al., 1984; Freund, 1985). Furthermore, I found that the temporal shift of SF preference in CRF response was observed regardless of the neuron's optimal SF (**Fig.6**). Considering those findings, the SF dynamics in cortical CRF response might reflect that of inputs from single type of LGN neurons. However, our estimation for the shift of SF preference is temporally too rough to lead a conclusion. Therefore, convergence of X and Y inputs (So and Shapley, 1979; Sestokas and Lehmkuhle, 1986) to single V1 neurons could not be ruled out. More detailed and systematic analyses are required.

SF tuning of CRF response in V1 neurons shifts through time from low SF to high SF,

and V1 neurons, whose optimal SF is low, have shorter latencies than that of neurons whose optimal SF is high. Then, CRF responses of V1 neurons realize “cause to fine” visual processing both in single neuron level and in population level.

2.4.3. Functions of the temporal property of surround suppression

I reported two components of surround suppression with distinct spatiotemporal property, early phase of surround suppression tuned to low SF and late phase of surround suppression tuned to high SF. What is the functional significance of this temporal change of SF tuning of surround suppression? Previous studies on the surround suppression have suggested that the suppressive field is critical for contrast gain control (Heeger, 1992; Carandine et al., 1997; Sadakane et al., 2005). A divisive gain control model applied to responses of V1 neurons was shown to increase independence of the responses of each neuron across neurons (Schwartz and Simoncelli, 2001). In addition, the surround suppression also increases stimulus-selectivity and optimizes filtering of stimulus features which may allow the efficient processing (Vingne and Gallant, 2002)

At early time window, surround suppression tuned low SF might reduce the response with a bias for low SF components in natural image, which mainly contains low SF (Simoncelli and Olshausen, 2001). The neuronal signals must be recorded into a de-correlated form of internal representation to improve efficiency. In the SF domain, the de-correlation is expressed as the flattening or “whitening” of the spatial power spectra of the neuronal signals, which is virtually a shift of information weight to high SF range. Then, to reduce low SF component by surround suppression improve efficiency of visual processing viewing in natural image. Furthermore, spatial extent of ECRF of V1 neuron is larger than that of CRF, then SF tuning of ECRF localizes to the region lower than that of CRF response. Because of this, surround

suppression hardly affects the peak SF of CRF response, and then, visual processing keep the “coarse to fine processing”. The late phase of surround suppression, tuned to the SF range that is high and close to the optimal SF for CRF response might have a significant in reducing redundancy inherent in response of the population of neurons.

Because the visual environment is consisted with high SF local components of visual objects which are imbedded in the global structure of low SF components, the early visual system would optimize the performance of information processing by changing the SF tuning property according to temporal phase of processing of the ceaselessly renewing visual world.

3. Psychophysical Study in Human

3.1. Introduction

What we see does not strictly reflect the physical characteristics of the different elements composing the visual scene, but the result of visual information processing which are optimized to achieve efficient and behaviorally appropriate representation of the visual world. Visual illusions reflect such optimized strategies of visual processing of the brain. Therefore, to clarify neural properties underlying the visual illusions is quite important for understanding essential mechanisms of visual information processing of the brain.

In this part, I focus on a visual illusion, “metacontrast”, which is supported to be a psychophysical correlate of the neuronal surround modulation in the visual system, and estimate the functional role of surround modulation in perceptual conscious level.

3.1.1. Psychophysical phenomena related to surround modulation

There are some types of psychophysical phenomena that are thought to be related to surround modulation in V1. That is, (1) Apparent contrast (Cannon et al., 1991,1996; Chubb et al., 1989; Ejima et al., 1985; Olzak et al., 1999; Solomon et al., 1998; Xing et al., 2000) (2) contrast detection threshold, and (3) visual saliency (Zhaoping and May, 2007). It is not clear whether the same mechanisms underlie these phenomena. However, in general, when the dependency on stimulus parameters observed in each of the three psychophysical phenomena is compared to that obtained in physiological studies on surround suppression, strong similarities in (a) location

or size dependency, (b) orientation or and/or spatial frequency (SF) dependency and (c) contrast dependency, are recognized. It is plausible the surround modulation, both suppressive and facilitatory enhances the perception of local differences and suppresses that of homogeneous texture, and that it is the key mechanism for the scene segmentation.

(1) Apparent contrast

The apparent contrast of a central grating embedded in an iso-oriented surround grating, the central stimulus is judged to be of a lower contrast than in the absence of the surround (Cannon et al., 1991, 1996; Chubb et al., 1989, Ejima et al., 1985; Xing et al., 2001). Similar to the suppressive modulation observed in V1 with identical sets of stimuli, (a) maximal effects occur when the center and the surround are of similar orientations and spatial frequencies (Cannon et al., 1991; Chubb et al., 1989) (b) Surround suppression increases when the contrast of the surround increases (Ejima et al., 1985; Xing et al., 2001), (c) surround suppression increases with the size of the surround stimulus over a large region of visual space (Ejima et al., 1985; Chubb et al., 1989). This effect is thought to play an important role in line completion, and in the extraction of degraded or incomplete contours.

(2) Contrast detection thresholds

Target detection is facilitated by the presence of collinear flank stimuli with the same orientation (Kapadia et al., 1995; Polat and Sagi, 1994, 2000; Solomon et al., 2000; Williams and Hess, 1998). As found facilitatory surround modulation in V1, contrast-detection thresholds varied depending on stimulus parameters. (a) These effects decrease when the relative orientation and distance between the stimuli increase and (b) when the degree of collinearity decreases, these effects decrease. This effect is thought to play a role in the discrimination of continuity and

discontinuity of visual objects.

(3) Visual saliency

The saliency of contours made of a number of oriented elements immersed in random texture depends on the (a) relative orientation and (b) separation of the contour elements (Beaudot and Mullen, 2001; Braun 1999; Field et al., 1993; Hess and Dakin 1997, 1999; Pettet, 1999; Robert et al., 2001). The rules governing the saliency of a contour immersed in a random texture are also reminiscent of the stimulus condition effective for surround modulation, e.g. orientation and spatial frequency.

3.1.2. Metacontrast

Metacontrast is one of the illusions in which the visibility of a briefly presented stimulus, the target (central stimulus), is reduced by another brief stimulus, the mask (surround stimulus), presented at the surround of the target. Metacontrast have similar spatial properties to the surround suppression observed in V1 neurons in the following points; (a) Spatial surrounding stimuli affect the response to center stimulus in metacontrast paradigm, the mask reduces the visibility of the target, (b) maximal effects are induced when the target and mask have same SFs, and (c) the effect increases when contrast of the surround stimulus increases. Metacontrast also shows an intriguing temporal characteristic, namely, that target visibility is reduced when a mask is presented simultaneously with or slightly after the target presentation. Therefore, metacontrast is termed as “visual backward masking”. Metacontrast is the good tool for examining the spatiotemporal properties of surround suppression, because, in this paradigm, not only spatial parameters (stimulus size, location, orientation, spatial frequency and contrast) but

also temporal parameter (SOA, stimulus onset asynchrony) could be systematically changed.

Previous studies examined psychophysical phenomena related to surround modulation, such as 1) apparent contrast, 2) contrast thresholds, and 3) visual saliency focused on the way of surround modulation encoding the “global” structures of visual field. From these studies, a great deal is known on the spatial properties, however, very little is known on the temporal properties of surround modulation. Knowledge of the spatial and temporal properties and their interaction of metacontrast will help us to understand neuronal basis of surround modulation, that is, how local visual signals are spatially and temporally integrated in the brain to generate global percepts. There are, however, few studies that have examined the suppressive effects of metacontrast by quantitatively and systematically changing the stimulus parameters of the target and mask in relation with stimulus onset asynchrony (SOA). In the present study, we used a circular sinusoidal grating patch for the target and sinusoidal grating annulus for the mask, and tested metacontrast by systematically changing the orientation, SF and contrast of the mask. To quantitatively evaluate the spatiotemporal properties of metacontrast is crucial to understand what is effectively represented in spatial and temporal context and to link the outputs of the neurons at early stages of cortical recording.

3.2. Methods

3.2. 1. Subjects

Five observers, the author (AI) and four others, who were naïve to the purposes of the experiments, served as subjects of the present study. The subjects' ages ranged from 20 to 23. All had normal or corrected-to-normal visual acuity. All procedures and protocol were approved by the Committee for the Protection of Human Subjects of the School of Health and Sport Sciences, Osaka University, and informed consent regarding the aim of the experimental procedures of the present study was obtained in writing from all the subjects.

3.2.2. Apparatus and stimuli

Visual stimuli were generated using a visual stimulation system VSG 2/3 (Cambridge Research System, England) controlled by an IBM-PC/AT-compatible computer and displayed on a CRT display (EIZO; Nanao, Japan; resolution, 1024 x 768 pixels; refresh rate, 100 Hz; mean background luminance, 30 cd/m²; screen size, 22.5 x 30° at a viewing distance of 57 cm). The stimulus consisted of a circular sinusoidal grating (target) of 2.3° diameter and a concentric sinusoidal grating annulus (mask) surrounding the target. The inner and outer diameters of the mask were 3° and 4.7°, respectively (**Figure 12**). Stimulus contrast was defined as

$$Contrast = (L_{max} - L_{min}) / (L_{max} + L_{min}),$$

where L_{max} and L_{min} respectively indicate the maximum and minimum luminances of the stimulus.

3.2.3 Procedure

All experiments were conducted in a room illuminated at a photopic level by overhead fluorescent lights. The subjects' eyes were adapted to this luminance level for 5 min. Before each experiment, the subject performed a block of practice trials in which the targets were presented to ensure that the subject could detect the targets. The stimulus sequence is shown in **Fig. 13**. A button press by the subject, whose head movements were restricted by a chin rest, initiated each trial. First, a fixation cross appeared at the center of the monitor. Then, after a delay of 1 sec, the stimuli were presented randomly at one of two locations, either 6.5° left or 6.5° right of the fixation cross, with varying stimulus onset asynchrony (SOA).

The duration of the target and mask presentation was 50 ms, and SOA was varied from -80 to +160 ms. The minus sign of SOA indicates that the mask appears first, followed by the target (paracontrast), and the plus sign indicates that the target appears first, followed by the mask (metacontrast). After the fixation cross and the stimuli disappeared, the subjects had to answer, using their psychophysical judgment, whether or not the target was visible by pressing a button. No feedback was provided. Half of the trials were catch trials to estimate the response biases of individual subjects, in which only the mask was presented. To prevent fatigue and visual adaptation, the subjects took a brief rest at least three times during a session of 90 minutes. Each stimulus condition consisted of a combination of SOA and a stimulus parameter, and 30 trials were conducted for each subject to obtain data. The stimulus condition was randomly changed from trial to trial.

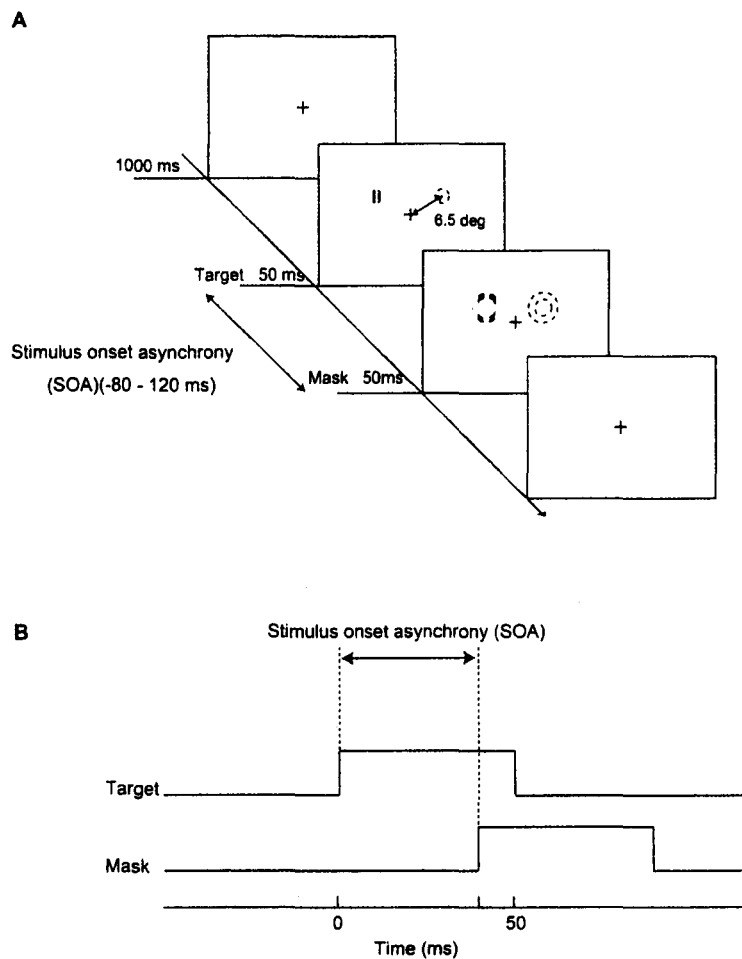


Figure 12

Stimulus sequence. First, the fixation cross appeared at the center of the monitor. After a delay of 1 sec, the stimuli were presented with varying SOA (-80 – 160 ms). The target was a circular grating 2.3° in diameter, and the mask was an annular grating with 3° and 4.7° inner and outer diameters, respectively. The target and mask were randomly presented in either the right or left visual field at a distance of 6.5° from the fixation cross.

3.2.4. Experiments

The experiments were designed to test the effects of changing the grating parameters, that is, orientation, SF, and luminance contrast. In all the experiments, the target was a circular sinusoidal grating with a vertical orientation, an SF of 2 c/deg and a contrast of 30 %. In Experiment 1, we tested the orientation dependency of metacontrast by varying the mask orientation, while keeping the contrast and SF of the mask fixed at 100 % and 2 c/deg, respectively. In Experiment 2, we tested the SF dependency by varying the mask SF, while keeping the mask orientation and contrast fixed at vertical and 100 %, respectively. In Experiment 3, we tested the contrast dependency by varying the mask contrast, while keeping the mask orientation and SF fixed at vertical and 2 c/deg, respectively. To check for a possible contamination of the results due to eye movement, the gaze direction and eye motion of the subjects were monitored with an eye-mark recorder (EMR-8, NAC Image Technology, Japan) during the experiments.

3.2.5. Data analysis

The masking effect was calculated as “100 – accuracy (%)” from the trials in which the target was presented. To quantify the tuning properties of metacontrast to grating parameters, the tuning data were fitted using the following functions for each parameter.

Orientation tuning

We fitted a Gaussian function to the tuning data to the orientation difference between the target

and mask. The equation for the Gaussian function is

$$M(OD) = Ke^{-((OD-\mu)/2\sigma)^2} + M_{base},$$

where M denotes the masking effect and OD denotes the orientation difference. K and σ are the amplitude and width of the Gaussian function, and μ is the orientation that evokes the maximal masking effect. M_{base} is the baseline of the curve. M_{base} , K , μ , and σ were optimized to provide the least-squares error of fit to the data. On the basis of the fitted curve, we determined the peak of the curve and the bandwidth of the orientation-tuning curve as a full width of the fitted Gaussian function at half height.

SF tuning

We fitted a difference of Gaussian (DOG) function to minimize the square error between the DOG curve and the obtained data for each SF of the mask (Xing, Ringach, Shapley, and Hawken, 2004). The fitted function is described as

$$M(sf) = K_a e^{-((sf-\mu_a)/2\sigma_a)^2} - K_b e^{-((sf-\mu_b)/2\sigma_b)^2} + M_{base},$$

where sf denotes the spatial frequency, and K_a and K_b are the integrated weights of the two Gaussian functions, and μ and σ are the mean and width of the Gaussian function, respectively. M_{base} is the baseline of the curve. M_{base} , K_a , K_b , μ_a , μ_b , σ_a , and σ_b , are all free parameters. On the basis of the fitted curve, we estimated the peak of the curve (peak SF) and SF tuning bandwidth. The bandwidth was calculated as

$$Bandwidth_{sf} = \log_2(SF_{high}/SF_{low}),$$

where SF_{high} and SF_{low} denote the SFs that produce 50 % of the peak SF on either side of the peak.

Contrast tuning

The Naka-Rushton equation was used to fit the masking effect as a function of contrast.

$$M(Cst) = M_{\max} Cst^n / (Cst_{50} + Cst^n)$$

Here, Cst denotes the mask contrast and M_{\max} the amplitude of scaling factor. The Cst_{50} is the medium value of M_{\max} . M_{\max} , Cst_{50} and n were optimized to provide the least-squares error of fit to the data.

3.3 Results

3.3.1. Experiment 1: Orientation dependency

We first asked how the masking effect depends on the orientation difference between the target and mask (**Figure 13**). In **Fig. 13A**, the accuracy of detecting the target, which is averaged across five subjects, is plotted as a function of SOA. In this test, we used two mask orientations that were identical to (iso-orientation) and orthogonal to (cross-orientation) that of the target. Since the false-positive responses to catch trials were rarely observed regardless of mask parameters (iso-orientation, $1.08 \% \pm 1.54 \%$; cross-orientation, $0.925 \% \pm 1.24 \%$ (mean \pm S.D.), $n = 5$), no correction was applied to the obtained data. Three important points emerged from this experiment. First, both masks yielded U-shaped masking functions with a trough bottom at 40 – 60 ms of SOA, that is, a typical type B metacontrast function (Kolers, 1962). Second, the masking effect was stronger for the iso-orientated mask than for the cross-oriented one at any SOAs. Third, the onset and effective range of SOA for masking were noticeably influenced by the mask orientation. The masking effect induced by the cross-oriented mask was observed in a narrow range of SOAs from 50 to 120 ms, whereas the iso-oriented mask was effective in a wide range from 0 to 120 ms. To further examine the tuning property of the masking effects to the orientation difference between the target and mask, we changed the mask orientation from 0 to 180° in 10° steps at SOAs of 0, 40, 60, and 80 ms, then calculated the “masking effect” as “100 – accuracy (%)”. **Figure 13B** shows the tuning curves of the masking effect to the orientation difference between the target and mask at four SOAs (0, 40, 60, and 80 ms). It is clearly demonstrated that, at all SOAs, the masking effect is maximal at orientation difference of zero and monotonically decreases as the orientation difference increases.

To compare the sharpness of the orientation-tuning curves, we normalized individual curves to the maximal masking effect (**Fig. 13C**). Here, it should be noted that the orientation-tuning curves became broader with an increase in SOA. To quantify the sharpness of the orientation tuning, we calculated the bandwidth at the half-height of the tuning curves for each SOA. The bandwidths were $29^\circ \pm 13^\circ$, $61^\circ \pm 14^\circ$, $89^\circ \pm 33^\circ$, and $149^\circ \pm 107^\circ$ (mean \pm S.D.) for SOAs of 0, 40, 60, and 80 ms, respectively, and significant differences were observed among the SOAs, except for SOA of 0 ms vs. 40 ms ($p < 0.05$; one-way ANOVA followed by Fisher's LSD post hoc test).

These results suggest that the masking effect consists of at least two components of the visual processing system with different temporal and orientation tuning characteristics. As the masking effect of the cross-oriented mask peaked at longer SOAs (40 – 80 ms, **Fig. 13A**) than that of iso-orientation, and the masking effect became less orientation-tuned with an increase in SOA (**Fig. 13C**), there seems to be a fast-conducting and less orientation-tuned pathway underlying metacontrast at long SOAs. The masking effect induced by short SOAs exhibited a sharp orientation tuning (**Fig. 13C**), suggesting an involvement of a slow-conducting and orientation-specific pathway.

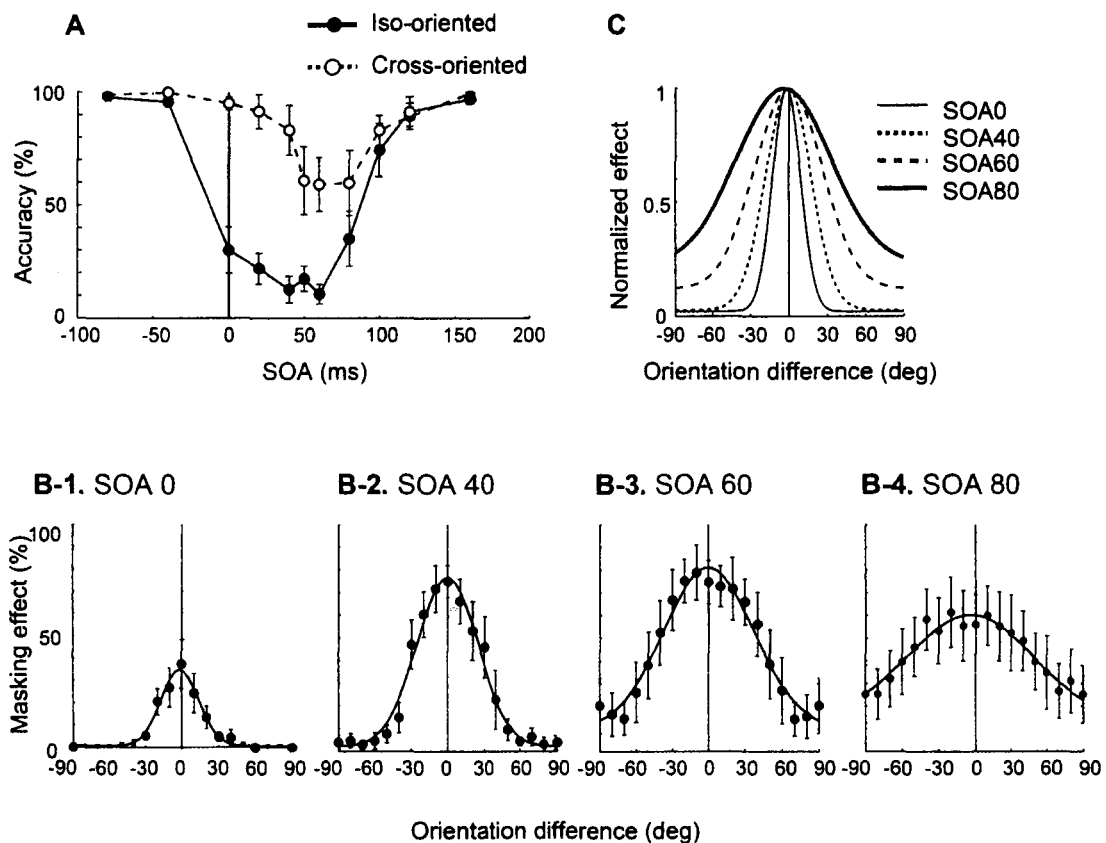


Figure 13

Effect of orientation difference between target and mask on metacontrast. (A) The accuracies (percentage of correct responses) of detecting a target with iso- (filled circles) and cross-oriented (open circles) masks were plotted as functions of SOA averaged across five subjects. The error bars indicate SEM. The target contrast was 30 % and mask contrast was 100 %. The SFs of the target and mask were 2 c/deg. (B) Tuning of masking effect to orientation differences at SOAs of 0 (B-1), 40 (B-2), 60 (B-3), and 80 ms (B-4). The orientation difference 0 was defined as the condition under which the target and mask had the same orientation. The masking effect was calculated as “100 – accuracy (%)”. The solid curve is a Gaussian function that best fits the data. C) Tuning curves for each SOA were normalized to the maximal masking effect.

3.3.2. Experiment 2: SF dependency

To examine how the masking effect depends on the SF of the mask, the detectability of a target with an SF of 2 c/deg was measured in the presence of the mask with three different SFs, that is, 0.4, 2, and 6 c/deg (**Figure 14**). The accuracy of target detection averaged across the five observers is shown in **Fig. 14A**. The false-positive responses to the catch trials were negligible ($0.91\% \pm 1.14\%$, $1.08\% \pm 1.54\%$ and $0.63\% \pm 0.36\%$ (mean \pm S.D.) for mask SFs of 0.4, 2 and 6 c/deg, $n = 5$). The result showed that the masking effect is strong at all SOAs when the mask SF is the same as the target SF (2 c/deg). The masks with SFs different from that of the target induced effects only at SOAs longer than 40 ms. These results indicate two things: First, the magnitude of the masking effect depends on the similarity of SFs between the target and the mask. Second, SF selectivity varies with SOA.

To examine SF selectivity in relation to SOA in detail, we tested the effects of twelve SFs of the mask grating: 0.2, 0.4, 0.8, 1, 1.5, 2, 2.5, 3, 4, 5, 6, and 8 c/deg (**Fig. 14B and C**). The SF tuning became broader with an increase in SOA. The bandwidths were 1.41 ± 0.63 , 2.1 ± 0.47 , 2.45 ± 0.82 , and 3.97 ± 1.2 (mean \pm S.D.) for SOAs of 0, 40, 60, and 80 ms, respectively. Significant differences were observed among the SOAs ($p < 0.05$; one-way ANOVA followed by Fisher's LSD post hoc test). Similarly to those of the orientation dependency experiment (Exp.1), these results suggest that the fast-conducting pathway underlying metacontrast at long SOAs is broadly SF-tuned; in contrast, the slow-conducting pathway underlying metacontrast at short SOAs is sharply SF-tuned. Another intriguing observation is the shift in the peak SFs that evoked the maximal masking effect. As shown in **Fig. 14B and C**, the peak SF decreased from high to low as SOA increased. Significant differences were observed among the SOAs except for SOA of 40 ms vs. 80 ms ($p < 0.05$; one-way ANOVA followed by Fisher's LSD post hoc

test). The peak SFs were 2.6 ± 0.23 , 2.49 ± 0.36 , 1.98 ± 0.78 , 1.49 ± 0.58 c/deg (mean \pm S.D) for SOAs of 0, 40, 60, and 80 ms, respectively. Thus, the slow-conducting pathway contributing to metacontrast at short SOAs is not only sharply SF-tuned but also relatively more sensitive to higher SFs (> 1 c/deg), and the fast-conducting pathway at long SOAs is broadly SF-tuned and more sensitive to lower SFs (< 1 c/deg).

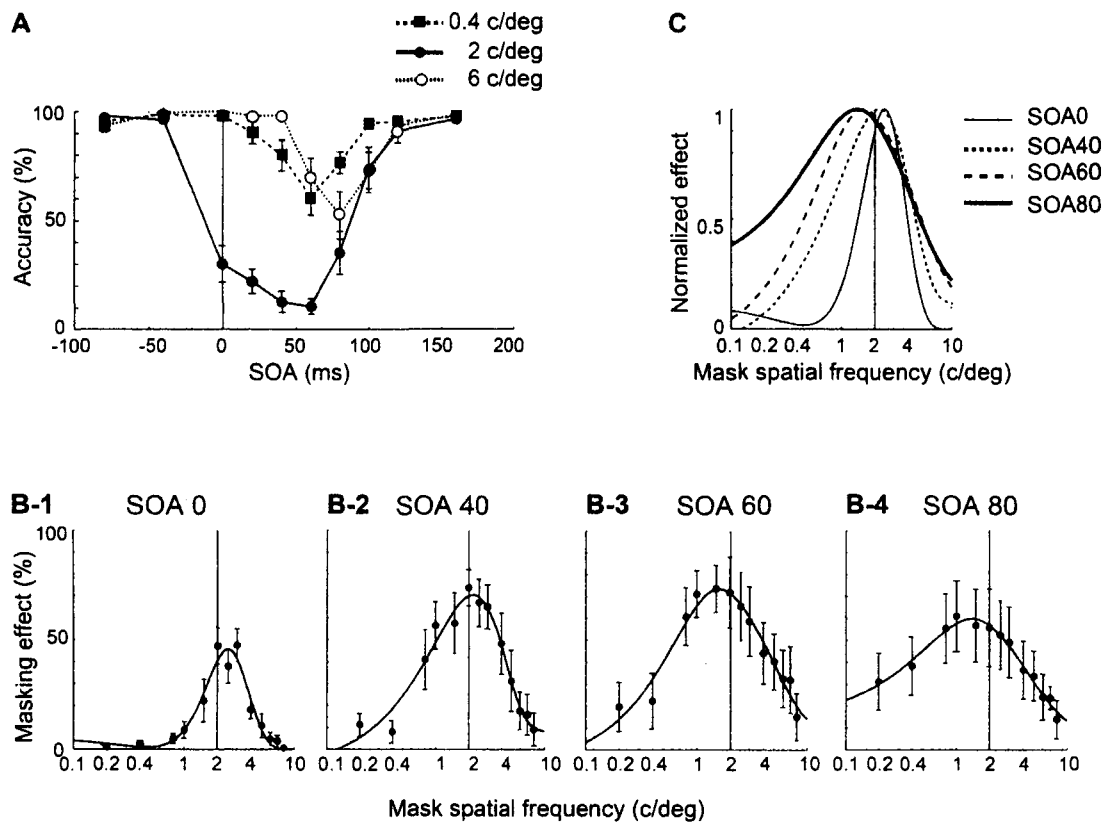


Figure 14

Effect of mask SF on metacontrast. (A) The effect of three masks with different SFs that were the same as (2 c/deg; filled circles), and lower (0.4 c/deg; filled squares), and higher (6 c/deg; open circles) than that of the target SF. The target contrast was 30 % and the mask contrast was 100 %. The orientations of the target and mask were vertical. (B) Tuning of masking effect to mask SF at SOAs of 0 (B-1), 40 (B-2), 60 (B-3) and 80 ms (B-4). Twelve SFs, 0.2, 0.4, 0.8, 1, 1.5, 2, 2.5, 3, 4, 5, 6, and 8 c/deg, were used for the mask. The solid curve is a difference of Gaussian function that best fits the data. (C) SF-tuning curves of masking normalized to maximal effect.

3.3.3. Experiment 3: Contrast dependency

In this section, we describe the dependency of the masking effect on mask contrast. In Experiment 3, we changed mask contrast, while we fixed other parameters of the target and mask at a vertical orientation and an SF of 2 c/deg. The target contrast was 30%. First, we measured the accuracy of the target detection when the mask and target had the same orientation and SF at three mask contrast, namely, 30, 60, and 100 % (**Fig. 15A**). False-positive responses to the catch trials were rarely observed regardless of the mask contrast (contrast 30 %, $3.05 \% \pm 3.73 \%$; 60 %, $2.05 \% \pm 2.98 \%$; 100%, $1.08 \% \pm 1.54 \%$ (mean \pm S.D.), $n = 5$). The magnitude of the masking effect increased as the mask contrast increased, and the difference in the strength of the masking effect was more prominent at short SOAs (0 – 20 ms) than that at long SOAs (40 – 80 ms). Next, we altered the mask contrast from 20 to 100 % in 10 % steps at SOAs of 0, 40, 60, and 80 ms (**Fig. 15B**). The contrast-masking curves obtained for each SOA exhibited distinctive features. At 0 ms of SOA (**Fig. 15B-1**), the contrast function of the masking effect showed a high contrast threshold, and at a contrast higher than 50 %, it increased monotonically without saturation. However, at an SOA of 80 ms (**Fig. 15B-4**), the contrast function showed a low contrast threshold, and it was saturated at contrasts higher than 50 %. Regarding the curves at SOAs of 40 and 60 ms that elicited the strongest masking effects, they exhibited profiles resembling the summation of the two curves for SOAs of 0 and 80 ms. These results again suggest that there are slow- and fast-conducting pathways underlying metacontrast. Slow metacontrast exhibits a low contrast sensitivity, a high orientation specificity and a high SF specificity, whereas fast metacontrast exhibits a high contrast sensitivity, a low orientation specificity and a low SF specificity.

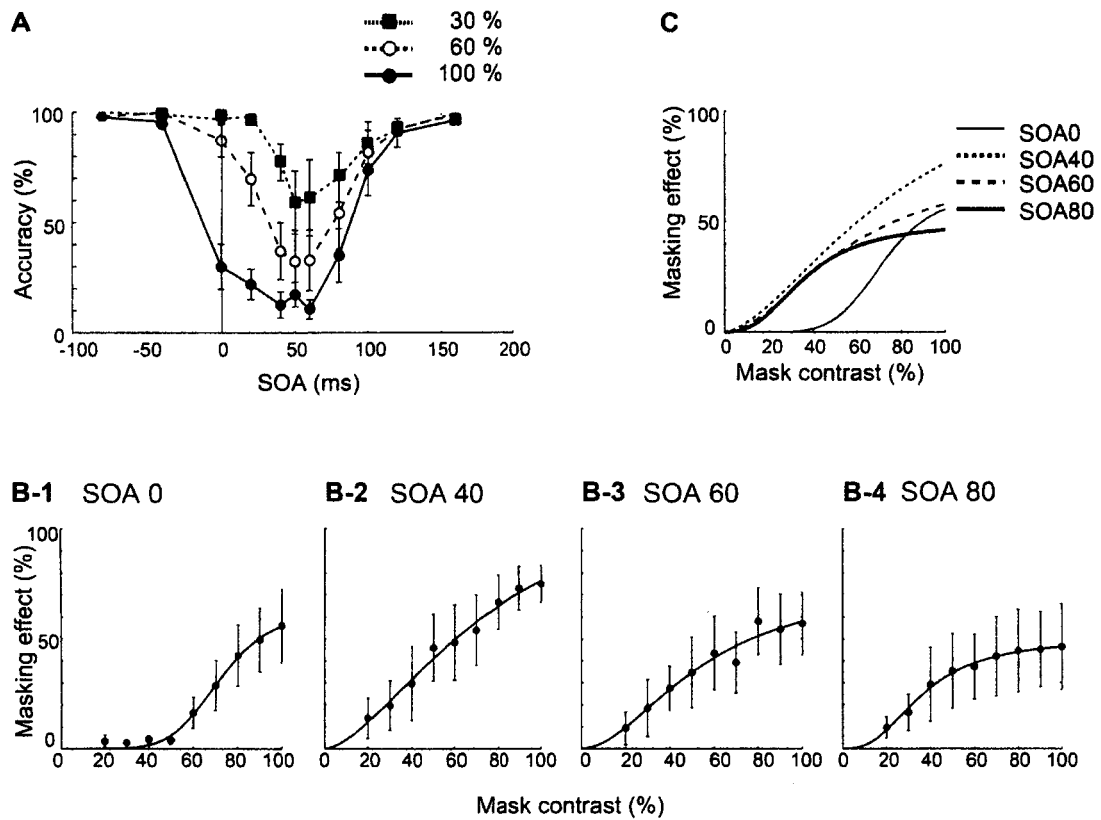


Figure 15

Effect of mask contrast on metacontrast. (A) The accuracies of detecting a target with masks with three different contrasts, 30 % (filled squares), 60 % (open circles), and 100 % (filled circles), were plotted as functions of SOA averaged across the five subjects. A target and a mask with the same orientation (vertical) and SF (2 c/deg) were used. (B) Contrast masking curves obtained for SOAs of 0 (B-1), 40 (B-2), 60 (B-3) and 80 ms (B-4) while changing mask contrast from 20 to 100 % in 10 % steps. The solid curve is a Naka-Rushton function that best fits the data. C) The superimposed contrast masking curves for SOAs of 0, 40, 60, and 80 ms.

3.3.4. Eye movements

To examine the possible involvement of eye movement in our results, we monitored the eye positions of three subjects using an eye-mark recorder. We recorded the eye positions under the conditions in which the mask was iso- and cross-oriented at SOAs of 0, 40, and 80 ms (Experiment 1). The subjects performed 30 trials under one condition. There was no consistent eye movement due to the appearance of stimuli under any stimulus conditions. The difference in the average eye position between 100 ms before and after the onset of the first stimulus was $0.18^\circ \pm 0.11^\circ$. There was no significant difference between iso- and cross-orientation conditions ($p = 0.63$, paired t-test) or among different SOA conditions ($p = 0.61$, one-way ANOVA). Therefore, eye movement explained neither the metacontrast effect nor its dependency on the stimulus feature of the mask.

3.4. Discussion

3.4.1. Properties of metacontrast

We examined the spatiotemporal characteristics of metacontrast using sinusoidal grating stimuli as the target and mask to quantitatively test the dependency of the masking effects on the stimulus features. We found three important properties of metacontrast. First, the magnitude of metacontrast was strongly dependent on the similarity of stimulus parameters, such as orientation and SF, between the target and mask (Figs. 12 and 13), which is in agreement with the results of previous studies (Werner, 1935; Rogowitz, 1983). Essentially, a strong masking effect was induced when the orientation and SF of the mask were identical to those of the target. This relationship of orientation selectivity was invariant with SOA. On the other hand, the most effective mask SF shifted from high (2.60 c/deg) to low (1.49 c/deg) as SOA increased from 0 ms to 80 ms (Fig. 14B and C). Second, the masking effect at long SOAs was broadly tuned to the orientation/SF difference between the target and mask stimuli, whereas that at short SOAs was narrowly tuned (Figs. 13 and 14). Third, the masking effect at long SOAs exhibited a high contrast sensitivity, whereas that at short SOAs exhibited a low contrast sensitivity, which is in agreement with Brietmeyer's previous observation (1981) that mask energy inducing the masking effect is lower under the conditions of long SOAs than under those of short SOAs. Taken together, these results suggest that there are distinct mechanisms with different spatiotemporal properties in the visual pathway underlying metacontrast; namely, the fast-conducting, less stimulus-specific and more contrast-sensitive mechanism contributes to metacontrast at long SOAs, and the slow-conducting, more stimulus-specific and less contrast-sensitive mechanism contributes to that at short SOAs.

3.4.2. Underlying mechanism of metacontrast

A general hypothesis on the underlying mechanism of metacontrast is that a mask-evoked neural response suppresses the response to a target, which reduces the perception of the target and raises its detection threshold. Our results suggest the existence of multiple components in the mask-induced neural response. Breitmeyer and Ganz (2000) explained metacontrast as an inhibitory interaction between two parallel pathways in the early visual system, namely, a faster magnocellular channel that generates a fast and transient response, and a slower parvocellular channel that generates a slow and sustained response (Merigan and Maunsell, 1993). According to their model, the target-induced slow and sustained response is suppressed by the mask-induced fast and transient response underlying metacontrast (interchannel interaction). On the other hand, when the target and mask are presented simultaneously, the target-induced fast and slow components of the response are suppressed by the corresponding component of the mask response (intrachannel interaction). If the metacontrast evoked in the present study is consistent with their hypothesis, the physiological correlates of the magno- and parvocellular systems should be reflected in the psychophysical properties of metacontrast. Therefore, we made a detailed comparison between our psychophysical evidence and previously known physiological evidence including the spatiotemporal properties of receptive fields (RFs), such as summation area (RF size), stimulus feature selectivity and center-surround interaction, along the hierarchy of information processing streams in order to investigate the locus and the circuitry underlying metacontrast.

The response of a neuron in the primary visual cortex (V1) to visual stimulation of its classical receptive field (CRF) is suppressed by a second stimulus concurrently presented in the

receptive field surround (ECRF) (Akasaki, Sato, Yoshimura, Ozeki and Shimegi, 2002; Blakemore and Tobin, 1972; DeAngelis, Freeman and Ohzawa, 1994; Jones, Grieve and Sillito, 2001; Knierim and van Essen, 1992; Li and Li, 1994; Nelson and Frost, 1978; Ozeki, Sadakane, Akasaki, Naito, Shimegi and Sato, 2004; Sceniak, Ringach, Hawken and Shapley, 1999; Sengpiel, Sen and Blakemore, 1997; Walker, Ohzawa and Freeman, 1999, 2000). This so-called contextual response modulation is a possible mechanism underlying metacontrast because of the similarity of properties between these two phenomena. First, metacontrast at short SOAs exhibits orientation specificity, which emerges at V1 but is obscure at subcortical levels, and contextual modulation also exhibits tuning to the orientation contrast between CRF and ECRF stimuli (Akasaki et al., 2002; DeAngelis et al., 1994; Li and Li, 1994; Ozeki et al., 2004). Second, the effect of metacontrast is maximal when the target and mask stimuli have the same orientation and SF, which is also true in physiological contextual modulation in V1 (Akasaki et al., 2002; DeAngelis et al., 1994; Knierim and Van Essen, 1992; Li and Li, 1994; Ozeki et al., 2004). Human brain imaging studies using functional magnetic resonance imaging (fMRI) (Zenger-Landolt and Heeger, 2003; Williams, Singh and Smith, 2003) and magnetoencephalography (Ohtani, Okamura, Yoshida, Yoyama and Ejima, 2002) in the visual cortex demonstrated that stimuli with center-surround configurations similar to those used in the present study suppress the center signals depending on the proximity of the stimulus features between the center and surround stimuli. A recent study has reported a good quantitative agreement between psychophysical responses and fMRI BOLD signals of V1 comparing with other visual areas such as V2 and V3 (Zenger-Landolt and Heeger, 2003). Third, the bandwidths of orientation and SF tuning curves of metacontrast (SOA0; orientation $29^\circ \pm 13^\circ$, SF, 1.41 ± 0.63 octave) are equivalent to those of V1 neurons of primates (De Valois, Albrecht and Thorell, 1982; De Valois, William and Hepler, 1982; Ringach, Shapley and Hawken, 2002). Thus, V1 is

a likely candidate locus of metacontrast (Macknik and Livingstone, 1998), although there is a study that failed to provide evidence of metacontrast effects in responses of single cells in monkey V1 and V2 (von der Heydt, Friedman, Zhou, Komatsu, Hanazawa and Murakami, 1997).

Next, we discuss the spatiotemporal properties of metacontrast in relation to the magno- and parvocellular systems. Our results suggest that there are, at least, two distinct components of the mask, that is, the fast conducting, less stimulus-specific and more contrast-sensitive mechanism for longer SOAs, and the slow-conducting, more stimulus-specific and less contrast-sensitive mechanism for shorter SOAs. These components of the masking effects with different time courses and stimulus specificities are attributable to the interaction either between the magno- and parvocellular pathways or between the phasic and sustained components of the neuronal response in the early visual system. A fast conductivity, relative effectiveness at lower SFs (**Fig. 14B and C**) and a high contrast sensitivity (**Fig. 15B and C**) are consistent with the properties of the magnocellular system, whereas a slow conductivity, effectiveness at higher SF (**Fig. 14B and C**) and a low contrast sensitivity (**Fig. 15B and C**) of the slow masking are consistent with those of the parvocellular system (Derrington and Lennie, 1984; Livingstone and Hubel; 1988, Merigan, Byrne and Maunsell; 1991a, Merigan, Katz and Maunsell, 1991b; Nowak, Munk, Girard and Bullier, 1995; Sclar, Maunsell and Lennie, 1990; Usrey and Reid, 2000; Winterkorn, Shapley and Kaplan; 1981, Xu, Ichida, Allison, Boyd and Bonds, 2001). Thus, our results support the idea of the different contributions of the magno- and parvocellular pathways to metacontrast with different temporal properties.

Rogowitz (1983) argued that mechanism underlying masking is an interchannel interaction, not intrachannel one, and the temporally nonoverlapping fast and slow components of a mask-induced response contribute to backward and forward maskings, respectively. This

hypothesis is based on the observation of little masking at an SOA of 0 ms when the intrachannel interaction was expected to be maximized, even though both the backward and forward maskings were clearly observed for positive and negative SOAs, respectively. In contrast, our results demonstrated that both the fast and slow components of mask-induced response with different spatiotemporal properties could contribute to the backward masking. The SOA-masking relationship exhibited a U-shaped backward masking function with a single trough, and the spatial properties such as stimulus-feature selectivity and contrast sensitivity varied continuously with change in SOA. These results suggest that the backward masking is evoked by two temporally overlapping two distinct components of a mask-induced response via intra- as well as interchannel interactions. Maunsell and Gibson (1992) suggested that both magno- and parvocellular inputs converge onto single V1 neurons, and that the visual responses of V1 neurons have mixed magno- and parvocellular components to a varying extent. There is evidence that the orientation tuning of V1 neurons develops with time after the onset of a response in both monkeys (Ringach, Hawken and Shapley, 1997) and cats (Pei, Vidyasagar, Volgushev, and Creutzfeldt, 1994). It has also been reported that SF tuning of V1 neurons in cats (Frazor, Albrecht, Geisler and Crane, 2004; Mazer, Vinje, McDermott, Schiller and Gallant, 2002) and monkeys (Bredfeldt and Ringach, 2002; Frazor et al., 2004) varies with time and the peak SF shifts from low to high along the time course of responses. Therefore, it is possible that the early component of neural responses predominantly contributes to fast metacontrast and the late component of neural responses contributes to slow metacontrast.

There is evidence that feedback inputs to V1 from higher order visual areas, such as MT, act on V1 neurons from the beginning of the V1 responses to flashing or moving visual stimulus (Hupe, James, Payne, Lomber, Girard and Bullier, 2001), and this feedback seems to play a role in perceptual figure/ground segregation (Hupe, James, Payne, Lomber, Girard and

Bullier, 1998). Therefore, it is possible that not only the bottom-up input but also the top-down one is involved in fast and slow metacontrasts. Further studies, in both humans and animals, are necessary to unmask the differential contribution of visual pathways to metacontrast with different time courses and stimulus specificities.

4. Conclusion

In this paper, I describe results that show the psychophysical and electrophysiological parallels between the effects of spatiotemporal surround suppression. Using sinusoidal grating patch and annulus as stimuli both experiments, it become possible to understand properties of surround suppression in a single neuron level and perception level, which have important function in contextual processing needs to be understood under natural viewing conditions. In electrophysiological experiments (**Section 2**), we recorded neurons in V1 and revealed temporal property of SF tuning of surround modulation. In psychophysical experiments (**Section 3**), I examined temporal properties of surround suppression at perceptual level using metacontrast paradigm, and revealed the temporal properties of orientation dependency, SF dependency and contrast sensitivity of metacontrast. The main finding is that there are temporal shift of surround modulation properties both in V1 neuron and metacontrast. These results suggest that contextual interaction, which reflect how visual information are integrated across space, change with time; firstly, global information is processed, and the fine and local visual information is processed later time.

4.1. Metacontrast and surround modulation in V1

We observed similarity between surround suppression properties of V1 neurons and metacontrast. 1) Maximal effects occur when the stimuli presented in center and surround regions have similar orientations and spatial frequencies (**Fig. 4A, Fig. 5A, Fig. 13, Fig. 14, and Fig. 15**). (2) Temporal shift of tuning of surround suppression have similar properties. Both in metacontrast (**Fig. 14C**) and surround suppression of V1 neurons (**Fig. 4, 5 and 6**), at early

phase of surround suppression, the SF tuning in suppression have low-pass type tuning, though time, the tuning become band-pass type tuning. However, some differences between surround modulation in V1 and metacontrast are also observed. One of the largest difference between surround suppression of V1 neurons and metacontrast in human perception is dependency of SOA. Several previous studies and my study indicate that metacontrast effect are never observed negative SOA and SOA, at which the largest effect was observed, depending on stimulus parameters, are around 40 – 80 ms (Fig. 13A, 14A, and 15A). I did not observe such dependency on SOA in surround suppression of V1 neurons. In surround suppression of V1 neurons, when changing SOA, the effect of suppression was observed both at positive SOAs positive and negative SOAs. Similar to previous study in V4 (Kondo et al., 2000), the strongest suppression for a total response was observe at SOA 0 condition (data are not shown). Underlying mechanisms in metacontrast is unknown, but suppression of activities in V1 has been viewed as a correlate of suppression in detection of stimulus, in term of the temporal shift of the surround suppression.

4.2. Function of temporal change of surround suppression

We observe similar tendency between temporal property of surround suppressions, which is observed in cat V1 neurons and human perception. Early phase of surround suppression tuned to low spatial frequency (SF) and had broad selectivity to stimulus features, whereas late phase of surround suppression tuned to high SF and high selectivity to stimulus features. What is a functional role of temporal change of surround suppression? Because the visual environment is consisted with high SF local components of visual objects which are imbedded in the global

structure of low SF components, the early visual system would optimize the performance of information processing by changing the SF tuning property according to the temporal phase of processing of the ceaselessly renewing visual world.

4.3. Bridging physiology and psychophysics

In this study, we observed surround suppression in response of a single neuron of cat V1 is collated with the perceptual visibility of a center stimuli change induced by the stimuli presented surround. In order to link the electrophysiological data of a single neuron and psychophysical results, I need to understand 1) how neuronal population responses are decoded to produce perceptual effect and 2) what the perceptual decision or the subject's performances will be. We could not know how neuronal population responses are decoded to produce perception and whether the V1 activities plays a functional role in the subject's conscious perception. Previous study showed that only minority of neurons in primary visual cortex show activity correlated with perception during binocular rivalry. Perceptual decisions involve processing in an extensive and incompletely hierarchy of cortical areas. From these reasons, it is impossible to simply link between properties of surround suppression of V1 neurons and those at perceptual level. However, electrophysiological and perceptual results on surround suppression might be conventionally linked by what we need to encode visual signals efficiently and meaningfully.

ACKNOWLEDGEMENTS

Many people have contributed to this dissertation, directly or indirectly, knowingly and unwittingly. I would like to take the opportunity to thank them.

I am grateful to my advisor, Hiromichi Sato, for generously providing the means, encouragement, and freedom to pursue this project. I thank Hiroyuki Kida and Hiroshi Sakamoto for their help in physiological recording.

I specially thank to Dr. Satoshi Shimegi for her inspiration and perspiration. I thank to Dr. Tomoyuki Naito, Dr. Osamu Sakakane. Dr. Hiroyuki Kida, Masahito Okamoto, Hironobu Osaki and Shinichiro Hara for valuable and funny discussions.

REFERENCE

Akasaki T., Sato H., Yoshimura Y., Ozeki H. Shimegi S. Suppressive effects of receptive field surround on neuronal activity in the cat primary visual cortex. *Neuroscience Research*, 43 (2002) 207-220

Allen E.A., Freeman R.D. Dynamic spatial processing originates in early visual pathways. *Journal of Neuroscience*, 26 (2006) 11763-74

Allison J.D., Bonds A.B. Inactivation of the infragranular striate cortex broadens orientation tuning of supragranular visual neurons in the cat. *Experimental Brain Ressearch*, 101 (1994) 415-426

Allman J., Miezin F., McGuinness E., Stimulus specific responses from beyond the classical receptive field: neurophysiological mechanisms for local-global comparisons in visual neurons. *Annual Review of Neuroscience*, 8 (1985) 407-430

Alpern M. Metacontrast; historical introduction. *American Journal of Optometry and Archives of American Academy of Optometry*, 43 (1952) 648-657

Anderson J.S., Lampl I., Gillespie D.C., Ferster D. Membrane potential and conductance changes underlying length tuning of cells in cat primary visual cortex. *Journal of Neuroscience*, 21 (2001) 2104-2112

Angelucci A., Levitt J.B., Lund J.S. Anatomical origins of the classical receptive field and modulatory surround field of single neurons in macaque visual cortical area V1. *Progress in Brain Research*, 136 (2002) 373-388

- Angelucci A, Sainsbury K. Contribution of feedforward thalamic afferents and corticogeniculate feedback to the spatial summation area of macaque V1 and LGN. *Journal of Comparative Neurology*, 498 (2006) 330-351
- Atick J.J. (1992) Could information theory provide an ecological theory of sensory processing? *Network: Computation in Neural Systems*, 3 213–251
- Atick J.J., Redlich A.N. (1992) Understanding retinal color coding from first principles. *Neural Computation*, 4 196 – 210
- Attneave, F. Information aspects of visual processing. *Psychological Review*, 61 (1954) 183–193
- Balow H. B. Possible principles underlying the transformation sensory message. In: *Sensory communication* (Rosenblith WA, ed). Cambridge MIT (1961)
- Bair W., Cavanaugh J.R., Smith M.A., Movshon J.A. The timing of response onset and offset in macaque visual neurons. *Journal of Neuroscience*, 22 (2002) 3189-205
- Bell A.J., Sejnowski T.J. The "independent components" of natural scenes are edge filters. *Vision Research*, 37 (1997) 3327-3338
- Beaudot W.H. and Mullen K.T. Processing time of contour integration: the role of color, contrast, and curvature. *Perception*, 30 (2001) 833–853
- Beaulier C., Somogyi P. Targets and Quantitative Distribution of GABAergic Synapses in the Visual Cortex of the Cat. *European Journal of Neuroscience*, 2 (1990) 296-303

Blakemore, C., Tobin, E. A.. Lateral inhibition between orientation detectors in the cat's visual cortex. *Experimental Brain Research*, 15 (1972) 439-440

Bonin V., Mante V., Carandini M. The suppressive field of neurons in lateral geniculate nucleus. *Journal of Neuroscience*, 25 (2005) 10844-10856

Bomds A.B. Role of inhibition in the specification of orientation selectivity of cells in the cat striate cortex. *Visual Neuroscience*, 2 (1989) 41-55

Bredfeldt C.E., Ringach D.L. Dynamics of spatial frequency tuning in macaque V1. *Journal of Neuroscience*, 22 (2002) 1976-1984

Braun J., On the detection of salient contours. *Spatial Vision*, 12 (1999) 211–225

Breitmeyer B.G. Metacontrast masking as a function of mask energy. *Bulletin of the Psychonomic Society*, 12 (1981) 50–52

Breitmeyer, B.G. Visual masking: An integration approach, *New York: Oxford University Press*. (1984)

Breitmeyer B.G., Ogmen H. Recent models and findings in visual backward masking: a comparison, review, and update. *Perception and Psychophysics*, 62 (2000) 1572-1595

Bullier J., Henry G.H. Neural path taken by afferent streams in striate cortex of the cat. *Journal of Neurophysiology*, 42 (1979) 1264-1270

Bullier J., Hupé J.M., James A.C., Girard P. The role of feedback connections in shaping the responses of visual cortical neurons. *Progress in Brain Research*, 134 (2001) 193-204.

Review.

Cannon, M.H., Fullenkamp, S.C. Spatial interactions in apparent contrast: Inhibitory effects among grating patterns, different spatial frequencies, spatial positions and orientations, *Vision Research*, 31 (1991) 1985–1998

Cannon, M.H., Fullenkamp, S.C. A model for inhibitory lateral interaction effects in perceived contrast. *Vision Research*, 36 (1996) 1115–1125

Cavanaugh J.R., Bair W., Movshon J.A. Selectivity and spatial distribution of signals from the receptive field surround in macaque V1 neurons. *Journal of Neurophysiology*, 88 (2002) 2547-2556

Cavanaugh J.R., Bair W., Movshon J. A. Nature and interaction of signals from the receptive field center and surround in macaque V1 neurons. *Journal of Neurophysiology*, 88 (2002) 2530-2546

Chen G., Dan Y., Li C.Y. Stimulation of non-classical receptive field enhances orientation selectivity in the cat. *Journal of Physiology*, 564 (2005) 233-243

Chubb C., Spelting G., Solomon J., Texture interactions determine perceived contrast. *The Proceedings of the National Academy of Sciences of the United States of America*, 86 (1989) 9631–9635

Common P. Independent component analysis, a new concept? *Signal Processing*, 36 (1994) 287

- 314

Carandini M., Heeger D. J. Summation and division by neurons in primate visual cortex.

Science, 264 (1994) 1333-1336

Creutzfeldt O. D., Kuhnt U., Benevento L. A., An intracellular analysis of visual cortical

neurones to moving stimuli: response in a co-operative neuronal network. *Experimental*

Brain Research, 21 (1974) 251-274

Crook J. M. Eysel Y.T., Machemer H.F. Influence of GABA-induced remote inactivation on

the orientation tuning of cells in area 18 of feline visual cortex: a comparison with area 17.

Neuroscience, 40 (1991) 1-12

Crook J.M., Kisvarday Z.F., Eysel U.T. GABA-induced inactivation of functionally

characterized sites in cat striate cortex: effects on orientation tuning and direction selectivity.

Visual Neuroscience, 14 (1997) 141-158

DeAngelis G.C., Freeman R.D., Ohzawa, I. Length and width tuning of neurons in the cat's

primary visual cortex. *Journal of Neurophysiology*, 71 (1994) 347 – 374

Derrington A.M., Fuchs A.F. Spatial and temporal properties of X and Y cells in the cat lateral

geniculate nucleus. *Journal of Physiology*, 293 (1979) 347-364

Derrington A.M., Lennie P. Spatial and temporal contrast sensitivities of neurones in lateral

geniculate nucleus of macaque. *Journal of Physiology (London)*, 357 (1984) 219-240

- De Valois R. L., Yund E.W., Hepler N. The orientation and direction selectivity of cells in macaque visual cortex. *Vision Research*, 22 (1982a) 531-544
- De Valois R.L., Albrecht D.G., Thorell L.G. Spatial frequency selectivity of cells in macaque visual cortex. *Vision Research*, 22 (1982b) 545-559
- Dragoi, V., Sharma, J., Sur, M., Dynamics of neuronal sensitivity in visual cortex and local feature discrimination. *Nature Neuroscience*, 5 (2992) 883 – 891
- Durand S., Freeman T.C., Carandini M. Temporal properties of surround suppression in cat primary visual cortex. *Visual Neuroscience*, 24 (2007) 679-690
- Ejima Y., Takahashi S., Apparent contrast of a sinusoidal grating in the simultaneous presence of peripheral gratings. *Vision Research*, 25 (1985) 1223–1232
- Emerson R.C., Gerstein G.L. Simple striate neurons in the cat. II. Mechanisms underlying directional asymmetry and directional selectivity. *Journal of Neurophysiology*, 40 (1977) 136-155
- Emerson R.C., Gerstein G.L. Simple striate neurons in the cat. I. Comparison of responses to moving and stationary stimuli. *Journal of Neurophysiology*, 40 (1977) 119-135
- Eysel U.T., Mücke T., Wörgötter F. Lateral interactions at direction-selective striate neurones in the cat demonstrated by local cortical inactivation. *Journal of Physiology*, 399 (1988) 657-675
- Ferster D., LeVay S. The axonal arborizations of lateral geniculate neurons in the striate cortex of the cat. *Journal of Comparative Neurology*, 182 (1978) 923-944

- Ferster D., Lindström S. An intracellular analysis of geniculo-cortical connectivity in area 17 of the cat. *Journal of Physiology*, 342 (1983) 181-215
- Field, D.J. Relation between the statistics of natural images and the response properties of cortical cells. *Journal of the Optical Society of America A*, 4 (1987) 2379–2394
- Field D.J., Hayes A. and Hess R.F., Contour integration by the human visual system: evidence for a local “association field. *Vision Research*, 33 (1993) 173–19
- Fisken R.A., Garey L.J., Powell T.P. The intrinsic, association and commissural connections of area 17 on the visual cortex. *Philosophical Transactions Royal Society London B Biological Science*, 272 (1975) 487-536
- Fitzpatrick D Seeing beyond the receptive field in primary visual cortex. *Current Opinion of Neurobiology*, 10 (2000) 438–443
- Freeman R.D., Ohzawa I., Walker G. Beyond the classical receptive field in the visual cortex. *Progress in Brain Research*, 134 (2001) 157-170
- Frazor R.A., Albrecht D.G., Geisler W.S., Crane A.M. Visual cortex neurons of monkeys and cats: temporal dynamics of the spatial frequency response function. *Journal of Neurophysiology*, 91 (2004) 2607-2627
- Freund T.F., Martin K.A., Smith A.D., Somogyi P. Glutamate decarboxylase-immunoreactive terminals of Golgi-impregnated axoaxonic cells and of presumed basket cells in synaptic contact with pyramidal neurons of the cat's visual cortex. *Journal of Comparative Neurology*, 221 (1983) 263-278

- Freund T.F., Martin K.A., Whitteridge D. Innervation of cat visual areas 17 and 18 by physiologically identified X- and Y- type thalamic afferents. I. Arborization patterns and quantitative distribution of postsynaptic elements. *Journal of Comparative Neurology*, 242 (1985) 263-274
- Gabbott P.L., Somogyi P. Quantitative distribution of GABA-immunoreactive neurons in the visual cortex (area 17) of the cat. *Experimental Brain Research*, 61 (1986) 323-331
- Gans L., Felder R. Mechanism of directional selectivity in simple neurons of the cat's visual cortex analyzed with stationary flash sequences. *Journal of Neurophysiology*, 51 (1984) 294-324
- Gilbert C.D. Microcircuitry of the visual cortex. *Annual Review of Neuroscience*, 6 (1983) 217-47
- Gilbert C.D., Wiesel T.N. Morphology and intracortical projections of functionally characterised neurones in the cat visual cortex. *Nature*, 280 (1979) 120-125
- Gilbert C.D., Wiesel T.N., Clustered intrinsic connections in at visual cortex. *Journal of Neuroscience*, 3 (1983) 1116–1133
- Gilbert A.D., Wiesel T.N., The influence of contextual stimuli on the orientation selectivity of cells in primary visual cortex of the cat. *Vision Research*, 30 (1990) 1689-1701
- Hata Y., Tsumoto T., Sato H., Tamura H. Horizontal interactions between visual cortical neurones studied by cross-correlation analysis in the cat. *Journal Physiology*, 441 (1991) 593-614

Hess R.F. and Dakin S.C., Absence of contour linking in peripheral vision. *Nature*, 390 (1997) 602–604

Hess R.F. and Dakin S.C., Contour integration in the peripheral field. *Vision Research*, 39 (1999) 947–959.

Hess R.H., Beaudot W.H.A., Kathy T.M., Dynamics of contour integration. *Vision Research*, 41 (2001) 1023-1037

Hicks T.P., Lee B.B., Vidyasagar T.R. The responses of cells in macaque lateral geniculate nucleus to sinusoidal gratings. *Journal Physiology*, 337 (1983) 183-200

Hicks T.P., Ruwe W.D., Veale W.L., Veenhuizen J., Aspartate and glutamate as synaptic transmitters of parallel visual cortical pathways. *Experimental. Brain Research*, 58 (1985) 421-425

Hubel D., Wiesel T., Receptive fields and functional architecture of monkey striate cortex. *Journal of Physiology* (London), 195 (1958) 215 - 243

Hubel D.H., Wiesel T.N. Cortical and callosal connections concerned with the vertical meridian of visual fields in the cat. *Journal of Neurophysiology*, 30 (1967) 1561-1573

Hupé J.M., James A.C., Girard P, Bullier J. Response modulations by static texture surround in area V1 of the macaque monkey do not depend on feedback connections from V2. *Journal of Neurophysiology*, 85 (2001) 146-163

Hupé J.M., James A.C., Girard P., Lomber S.G., Payne B.R., Bullier J. Feedback connections act on the early part of the responses in monkey visual cortex. *Journal of Neurophysiology*, 85 (2001) 134-145

Hupé J.M., James A.C., Payne B.R., Lomber S.G., Girard P., Bullier J. Cortical feedback improves discrimination between figure and background by V1, V2 and V3 neurons. *Nature*, 394 (1998) 784-787

Innocenti G.M., Fiore L. Post-synaptic inhibitory components of the responses to moving stimuli in area 17. *Brain Research*, 80 (1974) 122-126

Ishikawa A., Shimegi S., Sato H., Metacontrast masking suggests interaction between visual pathways with different spatial and temporal properties. *Vision Research*, 40 (2005) 2130–2138

Irvin G.E., Casagrande V.A., Norton T.T. Center/surround relationships of magnocellular, parvocellular, and koniocellular relay cells in primate lateral geniculate nucleus. *Visual Neuroscience*, 10(1993) 363-373

Jones H.E., Andolina I.M., Oakely M.M., Murphy P.C., Sillito A.M. Spatial summation in lateral geniculate nucleus and visual cortex. *Experimental Brain Research*, 135 (2000) 279-284

Jones H.E., Grieve K.L., Wang W., Sillito A.M. Surround suppression in primate V1. *Journal of Neurophysiology*, 86 (2001) 2011-2028

Kaplan E, Shaply R. M., X and Y cells in the lateral geniculate nucleus of macaque monkeys.

Journal of Physiology, 330 (1982) 125-143

Kapadia M.K., Ito M., Gilbert C.D., Westheimer G. Improvement in visual sensitivity by changes in local context: parallel studies in human observers and in V1 of alert monkeys.

Neuron, 15 (1995) 843-856

Kisvarday Z.F., Martin K.A. C., Frund T.F., Magloczky Z., Whitteridge D., Somogyi P.,

Synaptic targets of HRP- filled layer 3 pyramidal cells in the cat striate cortex, *Experimental Brain Research*, 64 (1986) 541 – 552

Kisvarday Z.F., Toth E., Rausch M., Eysel U.T. Orientation specific relationship between populations of excitatory and inhibitory lateral connection in the visual cortex of the cat,

Cerebral Cortex, 7 (1997) 695 – 618

Knierim J.J., van Essen D.C. Neuronal responses to static texture patterns in area V1 of the alert macaque monkey. *Journal of Neurophysiology*, 67 (1992) 961-980

Kolers P.A. Intensity and contour effects in visual masking. *Vision Research*, 2 (1962) 277-294

Kolers P.A., Rosner B.S. On visual masking (metacontrast): dichoptic observation. *American Journal of Psychology*, 73 (1960) 2-21

Kondo H, Komatu H., Suppression on neuronal responses by a metacontrast masking stimulus in monkey V4. *Neuroscience*, 36 (2000) 27 –33

Levick W.R. Another tungsten microelectrode. *Medical Biological Engineering*, 10(1972) 510-515

- Levitt J.B., Lund J.S. Contrast dependence of contextual effects in primate visual cortex. *Nature*, 387(1997) 73-76
- Li C.Y., He Z. J. Effects of patterned backgrounds on responses of lateral geniculate neurons in cat. *Experimental Brain Research*, 67 (1987) 16-26
- Li C.Y., Li W. Extensive integration field beyond the classical receptive field of cat's striate cortical neurons-classification and tuning properties. *Vision Research*, 34 (1994) 2337-2355
- Livingstone M.S., Hubel D.H. Segregation of form, color, movement, and depth: anatomy, physiology, and perception. *Science*, 240 (1988) 740-749
- Macknik S.L., Livingstone, M.S. Neuronal correlates of visibility and invisibility in the primate visual system. *Nature Neuroscience*, 1 (1998) 144-149
- Maffei L., Fiorentini A. The unresponsive regions of visual cortical receptive fields. *Vision Research*, 16 (1976) 1131-1139
- Martin K.A.C., Whitteridge D., Form, function and intracortical projections of spiny neurons in the striate cortex of the cat, *Journal of Physiology. (London)*, 353 (1984) 463–504.
- Maunsell J. H., Gibson J.R. Visual response latencies in striate cortex of the macaque monkey. *Journal of Neurophysiology*, 68 (1992) 1332-1344
- Mazer J.A., Vinji W.E., McDermotto J., Schiller P.H., Gallant J.L. Spatial frequency and orientation tuning dynamics in area V1. *The Proceedings of the National Academy of Sciences of the United States of America*, 99 (2002) 1645-1650

McGuire D.A., Gilbert C.D., Rivlin P.K., Wiesel T.N., Targets of horizontal connections in macaque primary visual cortex. *Journal of Comparative Neurology*, 305 (1991) 370 – 392

Meese T.S., Hess R.F. Low spatial frequencies are suppressively masked across spatial scale, orientation, field position, and eye of origin. *Journal of Vision*, 4 (2004) 843 - 59

Merigan W.H., Byrne C.E., Maunsell J.H. Does primate motion perception depend on the magnocellular pathway? *Journal of Neuroscience*, 11 (1991a) 3422-3429

Merigan W.H., Katz L.M., Maunsell, J.H. The effects of parvocellular lateral geniculate lesions on the acuity and contrast sensitivity of macaque monkeys. *Journal of Neuroscience*, 11 (1991b) 994-1001

Merigan W.H., Maunsell J.H. How parallel are the primate visual pathways? *Annual Review of Neuroscience*, 16(1993) 369-402

Morrone M.C., Burr D.C., Maffei L., Functional implications of cross-orientation inhibition of cortical visual cells. I. Neurophysiological evidence. *Proceedings Royal Society of London B Biological Science*, 216 (1982) 335-354

Mullikin W.H., Jones J.P., Palmer L.A. Receptive-field properties and laminar distribution of X-like and Y-like simple cells in cat area 17. *Journal of Neurophysiology*, 52 (1984) 350-371

Murphy P.C., Duckett S.G., Sillito A.M. Comparison of the laminar distribution of input from areas 17 and 18 of the visual cortex to the lateral geniculate nucleus of the cat. *Journal of Neuroscience*, 20 (2000) 845-853

Murphy P.C., Duckett S.G., Sillito A. M. Feedback connections to the lateral geniculate nucleus and cortical response properties. *Science*, 286 (1999) 1552-1554

Murphy P.C., Sillito A.M. Functional morphology of the feedback pathway from area 17 of the cat visual cortex to the lateral geniculate nucleus. *Journal of Neuroscience*, 16 (1996) 1180-1192

Naito T., Sadakane O., Okamoto M., Sato H. Orientation tuning of surround suppression in lateral geniculate nucleus and primary visual cortex of cat. *Neuroscience*, 23 (2007) 962-975

Nelson J. I., Frost B. J. Orientation-selective inhibition from beyond the classic visual receptive field. *Brain Research*, 139 (1978) 359-365

Nishimoto S., Arai M., Ohzawa I. Accuracy of subspace mapping of spatiotemporal frequency domain visual receptive fields. *Journal of Neurophysiology*, 93 (2005) 3524-3536

Nowak L.G., Munk M.H., Girard P., Bullier J. Visual latencies in areas V1 and V2 of the macaque monkey. *Visual Neuroscience*, 12 (1995) 371-384

Ogmen H. A neural theory of retino-cortical dynamics. *Neural Network*, 6 (1993) 245-273

Ogmen H., Breitmeyer B.G., Melvin R. The what and where in visual masking. *Vision Research*, 43 (2003) 1337-1350

Ohtani Y., Okamura S., Yoshida Y. Toyama K., Ejima Y. Surround suppression in the human visual cortex: an analysis using magnetoencephalography. *Vision Research*, 42 (2002) 1825-1835

- Oja E. A simplified neuron model as a principal component analyzer. *Journal of Mathematical Biology*, 15 (1982) 267 - 273
- Olzak L. A., Laurinen P. I., Multiple gain control processes contrast-contrast phenomena. *Vision Research*, 39 (1999) 3983-3987
- Ozeki, H. Sadakane, O. Akasaki, T. Naito, T., Shimegi, S., Sato, H. Relationship between excitation and inhibition underlying size tuning and contextual response modulation in the cat primary visual cortex. *Journal of Neuroscience*, 24 (2004) 1428–1438
- Pei X., Vidyasagar T.R., Volgushev M., Creutzfeldt O.D. Receptive field analysis and orientation selectivity of postsynaptic potentials of simple cells in cat visual cortex. *Journal of Neuroscience*, 14 (1994) 7130-7140
- Pettet M.W. Shape and contour detection. *Vision Research*, 39 (1999) 551–557.
- Polat U., Mizobe K., Pettet M. W., Kasamatsu T., Norcia A. M. Collinear stimuli regulate visual responses depending on cell's contrast threshold. *Nature*, 391(1998) 580-584
- Polat U. and Sagi D. Lateral interactions between spatial channels: suppression and facilitation revealed by lateral masking experiments. *Vision Research*, 33 (1993) 993–999
- Polat U. and Sagi D. The architecture of perceptual spatial interactions. *Vision Research*, 34 (1994) 73–78.
- Priebe N.J., Ferster D. Mechanisms underlying cross-orientation suppression in cat visual cortex. *Nature Neuroscience*, 9 (2006) 552-561

- Renagel P., Zador A.M. Natural scene statistics at the center of gaze. *Network*, 10 (1999) 341–350
- Ringach D.L., Bredfeldt C.E., Shapley R.M., Hawken M.J. Suppression of neural responses to nonoptimal stimuli correlates with tuning selectivity in macaque V1. *Journal of Neurophysiology*, 87 (2002) 1018-1027
- Ringach D.L., Hawken M.J., Shapley, R. Dynamics of orientation tuning in macaque primary visual cortex. *Nature*, 387 (1997) 281-284
- Rodieck R.W., Stone J. Analysis of receptive fields of cat retinal ganglion cells. *Journal of Neurophysiology*, 28 (1965) 832-849
- Rogowitz B. E. Spatial/temporal interactions: backward and forward metacontrast masking with sine-wave gratings. *Vision Research*, 23 (1983) 1057-1073
- Sadakane O., Ozeki H., Naito T., Akasaki T., Kasamatsu T., Sato H. Contrast-dependent, contextual response modulation in primary visual cortex and lateral geniculate nucleus of the cat. *European Journal of Neuroscience*, 23 (2006) 1633-1642
- Sato H, Katsuyama N, tamura H, Hata Y, Tsumoto T. Mechanisms underlying direction selectivity of neurons in the primary visual cortex of the macaque. *Journal of Neurophysiology*, 74 (1995) 1382-1394
- Sanger T.D. Optimal unsupervised learning in a single-layer linear feedforward neural network. *Neural Networks*, 2 (1989) 459 – 473
- Sceniak M.P., Ringach D.L., Hawken M.J., Shapley R. Contrast's effect on spatial summation by macaque V1 neurons. *Nature Neuroscience*, 2 (1999) 733-739

- Schiller P.H. Metacontrast interference as determined by a method of comparisons. *Perceptual and Motor Skills*, 20 (1965) 279-285
- Schiller P.H. Single unit analysis of backward visual masking and metacontrast in the cat lateral geniculate nucleus. *Vision Research*, 8 (1968) 855-866
- Sclar G., Maunsell J.H., Lennie P. Coding of image contrast in central visual pathways of the macaque monkey. *Vision Research*, 30 (1990) 1-10
- Sengpiel F., Sen A., Blakemore C. Characteristics of surround inhibition in cat area 17. *Experimental Brain Research*, 116 (1997) 216-228
- Sestokas A.K., Lehmkuhle S. Visual response latency of X- and Y-cells in the dorsal lateral geniculate nucleus of the cat. *Vision Research*, 26 (1986) 1041-1054
- Smith M. A. Bair W., Movshon J.A. Dynamics of suppression in macaque primary visual cortex. *Journal of Neuroscience*, 26 (2006) 4826-4834
- Sillito A.M., Cudeiro J., Murphy P. C. Orientation sensitive elements in the corticofugal influence on center-surround interactions in the dorsal lateral geniculate nucleus. *Experimental Brain Research*, 93 (1993) 6-16
- Sillito A.M., Grieve K.L., Jones H.E., Cudeiro J., Davis J. Visual cortical mechanisms detecting focal orientation discontinuities. *Nature*, 378 (1995) 492-496
- Sillito A.M., Jones H.E. Corticothalamic interactions in the transfer of visual information. *Philosophical Transaction Royal Society London B Biological Science*, 357 (2002) 1739-1752 Review

- Simoncelli, E.P. Olshausen, B. A. natural image statistics and neural representation. *Annual Review of Neuroscience*, 24 (2001) 1193 – 1216
- So Y.T., Shapley R., Spatial properties of X and Y cells in the lateral geniculate nucleus of the cat and conduction velocities of their inputs. *Experimental Brain Research*, 36 (1979) 533-550
- Solomon .A. and Morgan M.J. Facilitation from collinear flanks is cancelled by non-collinear flanks. *Vision Research*, 40 (2000) 279–286
- Solomon S.G., Peirce J.W., Lennie P. The impact of suppressive surrounds on chromatic properties of cortical neurons. *Journal of Neuroscience*, 24 (2004) 148-160
- Solomon S.G., Sur H, Lee B.B. Extraclassical receptive field properties of parvocellular, magnocellular, and koniocellular cells in the primate lateral geniculate nucleus. *Journal of Neuroscience*, 22 (2002) 338 – 349
- Sun C, Chen X, Huang L, Shou T. Orientation bias of the extraclassical receptive field of the relay cells in the cat's dorsal lateral geniculate nucleus. *Neuroscience*, 125 (2004) 495-505
- Skottun B.C., Grosf D.H., De Valois R.L. Responses of simple and complex cells to random dot patterns: a quantitative comparison. *Journal of Neurophysiology*, 59 (1988) 1719-1735
- Ts'o D.Y., Gilbert C.D., Wiesel T.N. Relationships between horizontal interactions and functional architecture in cat striate cortex as revealed by cross-correlation analysis. *Journal of Neuroscience*, 6 (1986) 1160-1170
- Tanaka K. Cross-correlation analysis of geniculostriate neuronal relationships in cats.

- Journal of Neurophysiology*, 49 (1983) 1303-1318.
- Tolhurst, D.J., Tadmor, Y., Chao, T. Amplitude spectra of natural images, *Optical and Physiological Optics*, 12 (1992) 229-232
- Usrey W.M., Reid R.C. Visual physiology of the lateral geniculate nucleus in two species of new world monkey: *Saimiri sciureus* and *Aotus trivirgatus*. *Journal of Physiology (London)*, 523 (2000) 755-769
- Van Essen D.C., Maunsell J.H.R., Hierarchical organization and functional streams in the visual cortex, *Trends Neuroscience*, 6 (1983) 370 – 375
- Van Hateren, J.H., Rouderman, D.L. Independent component analysis of natural image sequences yields spatio-temporal filters similar to simple cells in primary visual cortex. *Proceedings of the Royal Society of London, series B, Biological Sciences*, 265 (1998) 2315 – 2320
- Volgushev M., Pei X., Vidyasagar T.R., Creutzfeldt O.D. Excitation and inhibition in orientation selectivity of cat visual cortex neurons revealed by whole-cell recordings in vivo. *Visual Neuroscience*, 10 (1993) 1151-1155
- von der Heydt R., Friedman H. S., Zhou H., Komatsu H., Hanazawa A., Murakami, I. Neuronal responses in monkey V1 and V2 unaffected by metacontrast. *Investigative Ophthalmology and Visual Science*, 38 (1997) (Suppl.) 2146 (Abstract)
- Walker G.A., Ohzawa I., Freeman R.D. Asymmetric suppression outside the classical receptive field of the visual cortex. *Journal of Neuroscience*, 19 (1999) 10536-10553

- Walker G.A., Ohzawa I., Freeman R.D. Suppression outside the classical receptive field. *Visual Neuroscience*, 17 (2000) 369 – 379
- Webb B.S., Dhruv N.T., Solomon S.G., Tailby C., Lennie P. Early and late mechanisms of surround suppression in striate cortex of macaque. *Journal of Neuroscience*, 25 (2005) 11666-11675
- Webb B.S., Tinsley C.J., Vincent C.J., Derrington A. M. Spatial distribution of suppressive signals outside the classical receptive field in lateral geniculated nucleus. *Journal of Neurophysiology*, 94 (2005) 1789–1797
- Weng C., Yeh C.I., Stoelzel C.R., Alonso J.M.. Receptive field size and response latency are correlated within the cat visual thalamus. *Journal of Neurophysiology*, 93 (2005) 3537-3547
- Werner H. Studies of contour I. Qualitative analysis. *American Journal of Psychology*, 47 (1935) 40-64
- Williams A.L., Singh K.D. Smith A.T. Surround modulation measured with functional MRI in the human visual cortex. *Journal of Neurophysiology*, 89 (2003) 525-533
- Williams C.B. and Hess R.F., Relationship between facilitation at threshold and suprathreshold contour integration. *Journal of the Optical Society of America A*, 15 (1998) 2046–2051
- Williams M.C., Breitmeyer B.G., Lovegrove W.J., Gutierrez C. Metacontrast with masks varying in spatial frequency and wavelength. *Vision Research*, 31 (1991) 017-2023
- Winterkorn J. M., Shapley R., Kaplan E. The effect of monocular paralysis on the lateral geniculate nucleus of cat. *Experimental Brain Research*, 42 (1981) 117-121

- Xing J., Heeger D.J., Center-surround interactions in foveal and peripheral vision. *Vision Research*, 40 (2000) 3065 - 3072
- Xing D., Ringach D. L., Shapley R., Hawken M.J. Correlation of local and global orientation and spatial frequency tuning in macaque V1. *Journal of Physiology*, 557 (2004) 923-933.
- Xing D., Shapley R.M., Hawken M.J., Ringach D.L., Effect of stimulus size on the dynamics of orientation selectivity in Macaque V1. *Journal of Neurophysiology*, 94 (2005) 799-812
- Xu X., Ichida J. M., Allison J.D., Boyd J.D., Bonds A.B. A comparison of koniocellular, magnocellular and parvocellular receptive field properties in the lateral geniculate nucleus of the owl monkey (*Aotus trivirgatus*). (*London*), 531 (2001) 203-218
- Yarbus A.L. Eye movement and vision. New York: Plenum. 13 (1967) 454-361
- Zhaoping, L., May K.A., Psychophysical tests of the hypothesis of a bottom-up saliency map in primary visual cortex. *Plos computationa biology*, 3 (2007) 616–633

Publication list

Original paper

Ayako Ishikawa, Satoshi Shimegi, Hiromichi Sato,

Metacontrast masking suggests interaction between visual pathways with different spatial and temporal properties. *Vision Research*, 46, 2130-2138, 2006.

Meeting abstract

(International)

Ayako Ishikawa, Satoshi Shimegi, Hiroyuki Kida, Hiromichi Sato Spatiotemporal dynamics of surround suppression in cat V1: spatial frequency dependency Vision Sciences Society 6th Annual Meeting 2006 I 56 Sarasota, U.S.A., May, 2006

Satoshi Shimegi, Hiroyuki Kida, Ayako Ishikawa, Hiromichi Sato Spatiotemporal dynamics of surround suppression in cat V1: orientation and stimulus diameter Vision Sciences Society 6th Annual Meeting 2006 I55 Sarasota, U.S.A., May, 2006

Ayako Ishikawa, Satoshi Shimegi, Hiroyuki Kida, Hiromichi Sato Spatiotemporal dynamics of surround suppression in cat V1: spatial frequency Society for Neuroscience annual meeting 2005 389.12 Washington D.C., U.S.A., Nov., 2005

Satoshi Shimegi, Hiroyuki Kida, Ayako Ishikawa, Hiromichi Sato Spatiotemporal dynamics of surround suppression in cat V1: orientation and stimulus diameter Society for Neuroscience annual meeting 2005 389.9 Washington D.C., U.S.A., Nov., 2005

Hiroyuki Kida, Satoshi Shimegi, Ayako Ishikawa, Hiromichi Sato Spatiotemporal dynamics of surround suppression in cat V1: stimulus location Society for Neuroscience annual meeting 2005 3889.14 Washington D.C., U.S.A. Nov., 2005

(Domestic)

石川理子、七五三木聡、木田裕之、佐藤宏道 Spatiotemporal dynamics of surround suppression in cat V1: spatial frequency 第28回神経科学大会 P1-198 横浜 2005

年 7 月

七五三木聡、木田裕之、石川理子、佐藤宏道 Spatiotemporal dynamics of surround suppression in cat V1: orientation-contrast P1-201 第 28 回神経科学大会 横浜 2005 年 7 月

木田裕之、七五三木聡、石川理子、佐藤宏道 Spatiotemporal dynamics of surround suppression in cat V1: stimulus location 第 28 回神経科学大会 P1-197 横浜 2005 年 7 月

石川理子、七五三木聡、木田裕之、佐藤宏道 Spatiotemporal dynamics of visual masking in cat V1: spatial frequency 第 82 回日本生理学会大会 3P030 仙台 2005 年 5 月

七五三木聡、木田裕之、石川理子、佐藤宏道 Spatiotemporal dynamics of visual masking in cat V1: orientation and stimulus diameter 第 82 回日本生理学会大会 3P029 仙台 2005 年 5 月

木田裕之、七五三木聡、石川理子、佐藤宏道 Spatiotemporal dynamics of visual masking in cat V1: stimulus location 第 82 回日本生理学会大会 3P022 仙台 2005 年 5 月

石川理子、木田裕之、七五三木聡、佐藤宏道 ネコ一次視覚野のニューロン活動と視覚マスキング 第 97 回近畿生理談話会 京都 2004 年 11 月

七五三木聡、木田裕之、石川理子、佐藤宏道 一次視覚野における刺激文脈依存的反応修飾の時間ダイナミクス 第 8 回視覚科学フォーラム 鳥取 2004 年 7 月

石川理子、七五三木聡、佐藤宏道 メタコントラストから推定さるヒトの並列視覚情報処理 第 96 回近畿生理談話会 京都 2003 年 8 月

石川理子、七五三木聡、佐藤宏道 メタコントラストからみたヒトの並列視覚情報処理 第 7 回視覚科学フォーラム 38 大阪 2003 年 7 月